



A proxy for all seasons? A synthesis of clumped isotope data from Holocene soil carbonates

Julia R. Kelson^{a, b, *}, Katharine W. Huntington^a, Daniel O. Breecker^c,
Landon K. Burgener^d, Timothy M. Gallagher^c, Gregory D. Hoke^e, Sierra V. Petersen^b

^a Department of Earth and Space Sciences, University of Washington, Seattle, WA, USA

^b Department of Earth and Environmental Sciences, University of Michigan, Ann Arbor, MI, USA

^c Department of Geological Sciences, University of Texas at Austin, Austin, TX, USA

^d Department of Marine, Earth, and Atmospheric Sciences, NC State University, Raleigh, NC, USA

^e Department of Earth Sciences, Syracuse University, Syracuse, NY, USA

ARTICLE INFO

Article history:

Received 14 January 2020

Received in revised form

27 February 2020

Accepted 28 February 2020

Available online xxx

Keywords:

Stable isotopes

Paleoclimatology

Global

Cenozoic

Holocene

ABSTRACT

Soil carbonates are important paleoclimate archives, but interpretations of their isotopic compositions ($\delta^{18}\text{O}$, $\delta^{13}\text{C}$, and Δ_{47}) are hampered by uncertainty in the annual timing of their accumulation. Several previous studies have inferred the annual timing of soil carbonate formation by comparing modern air/soil temperatures with temperatures estimated from the clumped isotopic composition ($T\Delta_{47}$) of Holocene soil carbonates. Here, we compile the existing Δ_{47} data to first consider if recent changes in Δ_{47} standardization methods alters the apparent seasonal biases. Then we explore the importance of various environmental parameters on soil carbonate $T\Delta_{47}$ and discuss implications for associated paleoclimate reconstructions. Most soil carbonates record $T\Delta_{47}$ values higher than mean annual air temperature, but the residual varies from -4 to $+24$ °C. Δ_{47} values for most observed soil profiles do not vary with depth. We find that the grain size of the soil matrix, timing of precipitation, and presence of vegetation each explain a portion of the observed variance in seasonal bias and can be used to aid in interpretations of $T\Delta_{47}$ values from paleosols. In some soil carbonates, a warm-season bias in $T\Delta_{47}$ is accompanied with calculated $\delta^{18}\text{O}$ values of soil water that appear to be biased toward the $\delta^{18}\text{O}$ of summer rainfall. Most estimated values of $\delta^{18}\text{O}$ of soil water are within 2‰ of the $\delta^{18}\text{O}$ values of mean annual rainfall. Where possible, paleoclimate reconstructions should consider precipitation timing, soil texture, and vegetation cover to aid in identifying the seasonal bias of soil carbonate stable isotopic compositions.

© 2020 Published by Elsevier Ltd.

1. Introduction

Soil carbonates are widespread in the geologic record and comprise an important archive of terrestrial paleoenvironments. The stable isotope composition of soil carbonates has been used extensively to investigate the evolution of habitats, ecology, climate, tectonics, and landforms. For example, past studies have used the carbon isotopic composition ($\delta^{13}\text{C}$) of soil carbonate to reconstruct changes in the composition of Cenozoic plant communities (e.g., the proportion of C3 and C4 vegetation; Cerling et al., 1989; Wang et al., 1993; Quade et al., 1995; Ding and Yang, 2000;

Monger et al., 2009; Levin et al., 2011), changes in atmospheric CO_2 concentrations throughout the Phanerozoic (e.g., Da et al., 2019; Ekart et al., 1999) and changes in soil respiration rates (Caves et al., 2016; Caves Rugenstein and Chamberlain, 2018). The oxygen isotopic composition of soil carbonates ($\delta^{18}\text{O}_c$) is commonly used to infer changes in local meteoric waters and/or local temperature (Behrensmeyer et al., 2007; Cerling and Hay, 1986; Dworkin et al., 2005; Fox and Koch, 2004; Garzione et al., 2000; Kaakinen et al., 2006; Koch et al., 1995; Liu et al., 1996; Monger et al., 1998; Nordt et al., 2003; Sikes and Ashley, 2007; Smith et al., 1993; Wang et al., 1996). More recently, clumped isotope thermometry (Δ_{47}) has provided the basis for estimating growth temperature of soil carbonates by using the temperature-dependent proclivity for ^{18}O and ^{13}C to bond in the same carbonate molecule. This estimate of temperature from Δ_{47} allows the worker to solve for $\delta^{18}\text{O}$ of growth water, enabling quantitative reconstruction of both temperature

* Corresponding author. Department of Earth and Environmental Sciences, University of Michigan, Ann Arbor, MI, USA

E-mail address: jrkelson@umich.edu (J.R. Kelson).

and $\delta^{18}\text{O}$ of meteoric waters with a single analysis. Δ_{47} analysis of paleosol carbonates has improved paleoaltimetry (Fan and Carrapa, 2014; Garzione et al., 2014; Huntington and Lechler, 2015; Ingalls et al., 2018; Lechler et al., 2013; Leier et al., 2013), expanded reconstructions of terrestrial temperatures and hydrology (Burgener et al., 2019; Eagle et al., 2013; Hyland et al., 2018; Kelson et al., 2018; Lechler et al., 2018; Methner et al., 2016; Page et al., 2019; Snell et al., 2013; Suarez et al., 2011; Tobin et al., 2014), advanced atmospheric $p\text{CO}_2$ reconstructions (Ji et al., 2018), and enabled characterization of habitats of human evolution (Passey et al., 2010).

Despite the versatility and value of the stable isotopic composition of soil carbonates, their formation process and its annual timing remains a topic of debate. Because the seasonal and diurnal range in surface temperature on land is generally much larger than the secular changes in temperature through geologic time that most studies of terrestrial paleoclimate wish to address, even slight changes in the seasonal bias of a terrestrial climate record must be recognized in order to interpret Δ_{47} , $\delta^{18}\text{O}$ and $\delta^{13}\text{C}$ values of soil carbonates (Breecker et al., 2009; Burgener et al., 2016; Gallagher et al., 2019; Gallagher and Sheldon, 2016; Hough et al., 2014; Huntington and Lechler, 2015; Huth et al., 2019; Oerter and Amundson, 2016; Peters et al., 2013; Ringham et al., 2016).

Previous workers have sought to constrain the annual timing of soil carbonate formation by comparing the clumped isotope temperature (here $T\Delta_{47}$) of Holocene soil carbonates to measured modern local temperatures (Burgener et al., 2018, 2016; Gallagher and Sheldon, 2016; Ghosh et al., 2006b; Hough et al., 2014; Huth et al., 2019; Passey et al., 2010; Peters et al., 2013; Quade et al., 2013, 2011; Ringham et al., 2016). However, varied seasonal biases are reported, and recent publications raise the possibility that analytical artifacts may explain some of the differences in seasonal bias. Here we systematically examine the previously published Δ_{47} data for Holocene soil carbonates to (1) account for possible artifacts in Δ_{47} standardization, (2) compare updated Δ_{47} temperatures to local mean annual temperatures to assess timing of formation, and (3) explore the importance of several environmental variables in controlling apparent timing of formation that could potentially be constrained in paleosols, including depth in soil column, timing of precipitation, vegetation cover, and soil texture. Lastly, we discuss implications for interpretations of isotopic values of paleosol carbonates in the geologic record.

2. Background: soil carbonate formation and isotopic composition

Pedogenic carbonates form in situ in arid to sub-humid environments (Birkeland, 1984; Jenny, 1941). The precipitation of carbonate in a soil is thought to be controlled by the interplay between soil water, soil temperature, and soil CO_2 (Arkley, 1963; Breecker et al., 2009; Drever, 1982; Gocke et al., 2012; Li et al., 2018; Marion and Schlesinger, 1994; McDonald et al., 1996; McFadden et al., 1991; Monger et al., 1991; Zamanian et al., 2016), assuming sufficient Ca^{2+} is available, either from dust or weathering of parent material (Birkeland, 1984; Gile et al., 1966; Harden et al., 1991; McFadden, 2013). Calcite can progressively accumulate over hundreds to millions of years given a stable geomorphic surface (Durand et al., 2010; Machette, 1985), usually as a result of precipitation, dissolution, and re-precipitation (Salomons and Mook, 1986; West et al., 1988). It is generally assumed that soil carbonates form when the solution in pore space reaches supersaturation with respect to calcite, but organic carbon can poison nucleation sites and can hamper calcite formation in natural soils (Inskeep and Bloom, 1986; Lebrón and Suárez, 1998; Marion et al., 2008; Suarez

and Šimůnek, 1997).

The $\delta^{13}\text{C}$ values of soil carbonates are controlled by the $\delta^{13}\text{C}$ of soil CO_2 , which is a mixture of biogenically-respired soil and atmospheric CO_2 (Amundson et al., 1988; Amundson and Lund, 1987; Breecker et al., 2009; Cerling et al., 1991; Cerling and Quade, 1993). In most soils, $\delta^{13}\text{C}$ values of soil carbonates decrease with depth (e.g., Cerling, 1984; Cerling and Quade, 1993; Quade et al., 1989). Seasonal biases of $\delta^{13}\text{C}$ are generally not considered, although seasonal variations in plant growth and soil respiration impart a seasonal bias in $\delta^{13}\text{C}$ of soil CO_2 in some calcic soils (Breecker et al., 2012).

Soil carbonate $\delta^{18}\text{O}$ values (here $\delta^{18}\text{O}_c$) are controlled by the oxygen isotope composition of soil water ($\delta^{18}\text{O}_{\text{sw}}$) and the temperature of mineral precipitation (Cerling, 1984; Cerling and Quade, 1993; Quade et al., 2007; Salomons and Mook, 1986). $\delta^{18}\text{O}$ values of soil water are primarily controlled by $\delta^{18}\text{O}$ values of rainfall (Gehrels et al., 1998; Tan et al., 2017), but can also be affected by evaporation in the near-surface (Allison et al., 1983; Barnes and Allison, 1983; Breecker et al., 2009; Hsieh et al., 1998; Huth et al., 2019; Liu et al., 1996; Oerter and Amundson, 2016; Oshun et al., 2015), as well as freezing, or storage and mixing with other local waters like snowmelt (Gazis and Feng, 2004; Sprenger et al., 2018; Tang and Feng, 2001). Agreement between $\delta^{18}\text{O}$ values of local meteoric waters (rivers or rain) and $\delta^{18}\text{O}_{\text{sw}}$ calculated from $\delta^{18}\text{O}_c$ and an assumed temperature (usually mean annual air temperature) has been observed, with little discussion of seasonal bias in $\delta^{18}\text{O}_c$ (Cerling and Quade, 1993; Hoke et al., 2013, 2009; Peters et al., 2013; Quade et al., 2007). In some locations, it has been demonstrated that the calculated $\delta^{18}\text{O}_{\text{sw}}$ is most similar to $\delta^{18}\text{O}$ values of meteoric waters (rain or soil water) from the assumed period of soil carbonate formation (Gallagher and Sheldon, 2016; Hough et al., 2014; Huth et al., 2019). These data suggest that $\delta^{18}\text{O}_c$ may be seasonally biased in some environments, not only because of temperature of formation, but also because of seasonal changes in the $\delta^{18}\text{O}$ value of soil waters.

The Δ_{47} value of a carbonate mineral is a thermodynamically based estimate of its growth temperature. Δ_{47} refers to a measurement of the abundance of $^{13}\text{C}-^{18}\text{O}$ bonds relative to their expected abundance if the isotopes were randomly distributed among isotopologues. $^{13}\text{C}-^{18}\text{O}$ bonds are more energetically favorable at lower temperatures, so their concentration can be used as a thermometer (Eiler, 2011, 2007; Ghosh et al., 2006a; Schauble et al., 2006). Assuming isotopic equilibrium is achieved, the Δ_{47} value of soil carbonate is controlled by the ambient temperature of the soil. To date, kinetic effects have only been detected in natural soil carbonates from cold environments that form through cryogenically induced precipitation (Burgener et al., 2018, 2016).

While Δ_{47} of soil carbonates records ambient soil temperature, it is often an estimate of air temperature that are sought after for paleoclimate purposes. The relationship between air and soil temperature can be quite complex. First, daily and seasonal fluctuations in air temperature are increasingly damped and lagged with depth as they propagate downward in the soil column, as described by heat diffusion equations (Hillel, 1982; Radcliffe and Šimůnek, 2010). These physics predict that daily fluctuations in soil temperature will be negligible by depths of approximately 50 cm, while seasonal fluctuations in soil temperature can be apparent at depths of >1 m (Hillel, 1982). Soil temperatures can be warmer than air temperatures due to radiative heating (Burgener et al., 2019; Cermak et al., 2017; Gallagher et al., 2019; Geiger et al., 2009; Kaufmann et al., 2003; Passey et al., 2010). Furthermore, the seasonal range in soil temperatures can be reduced by the presence of vegetation and snow (Gallagher et al., 2019). These soil physics led to the prediction that the Δ_{47} value of soil carbonates

should depend on the timing and depth of formation (Peters et al., 2013; Quade et al., 2013, 2007).

2.1. Seasonal bias of soil carbonate formation from previous studies of Δ_{47}

Comparisons between environmental conditions (e.g., air and soil temperature) and Δ_{47} values of Holocene soil carbonates have been made in various settings with the purpose of deciphering seasonal biases of carbonate formation (Fig. 1; Burgener et al., 2018, 2016; Gallagher and Sheldon, 2016; Hough et al., 2014; Huth et al., 2019; Passey et al., 2010; Peters et al., 2013; Quade et al., 2013, 2011; Ringham et al., 2016). Initial observations suggested that carbonate formation is warm-season biased: Δ_{47} values were similar to peak summer temperatures or even hotter, interpreted to be due to radiative solar heating of the ground surface (Breecker et al., 2009; Burgener et al., 2016; Hough et al., 2014; Passey et al., 2010; Peters et al., 2013; Quade et al., 2013; Ringham et al., 2016). As a result of these initial studies, the assumption made in the vast majority of paleoclimate studies is that soil carbonate Δ_{47} temperatures are warm season biased. However, some observations showed that soil carbonates in some localities yield growth temperatures similar to mean annual temperature (Burgener et al., 2016; Gallagher and Sheldon, 2016; Peters et al., 2013). These studies of Δ_{47} in Holocene soil carbonates point to a need to re-evaluate the predominant assumption that soil carbonates form in the warm season, and the opportunity to evaluate environmental factors that could be used to predict seasonal bias in pre-Holocene samples.

Each of the above studies developed hypotheses to explain site-specific Δ_{47} temperatures. First, depth in the soil column was originally predicted to control Δ_{47} (Quade et al., 2013), but a systematic depth-dependency in Δ_{47} was not supported by subsequent data (Ringham et al., 2016; Burgener et al., 2016). The importance of hydrology and the timing of rain/snow events has been identified as a possible control on soil carbonate formation in

several studies. Differences in rainfall seasonality were used to explain the variation in Δ_{47} bias in the Andes of Argentina (Peters et al., 2013), while timing of snow melt was invoked to explain Δ_{47} values similar to MAAT at high altitudes in the Chilean Andes (Burgener et al., 2016). Huth et al. (2019) hypothesized that large water infiltration events promote soil carbonate formation, leading to a summer bias in soil carbonate formation in Utah. Soil texture was invoked to explain the timing of carbonate formation by modulating the rate of change in soil moisture: fine-grained soils (silt or finer) retain moisture, while coarse-grained soils (sand or coarser) dry relatively quickly after rain events (Blodgett, 1988; Bouma and Bryla, 2000; Burgener et al., 2018). The timing of plant growth has been hypothesized to control the timing of carbonate formation as plants uptake water (Meyer et al., 2014), but Δ_{47} evidence for this effect was not conclusive (Ringham et al., 2016). The presence of plant cover can reduce radiative heating and has been hypothesized to reduce soil temperatures (Burgener et al., 2019; Gallagher et al., 2019; Passey et al., 2010).

Put together, these studies suggest varied seasonal bias in soil carbonate formation, and varied levels of importance of the following factors in determining soil carbonate Δ_{47} values: depth in soil column, timing and phase of precipitation, soil texture, and vegetative cover. Here we evaluate if the reported biases and patterns are upheld when the Δ_{47} data is reprocessed with modern data standards, then we explore the universality of various environmental factors in the global dataset of recalculated Δ_{47} temperatures.

3. Methods

3.1. Datasets considered

We compiled all studies that have published Δ_{47} (and concurrent $\delta^{13}\text{C}$, $\delta^{18}\text{O}$ measurements) of Holocene soil carbonates that are accompanied by meteorological data from in situ monitoring and/

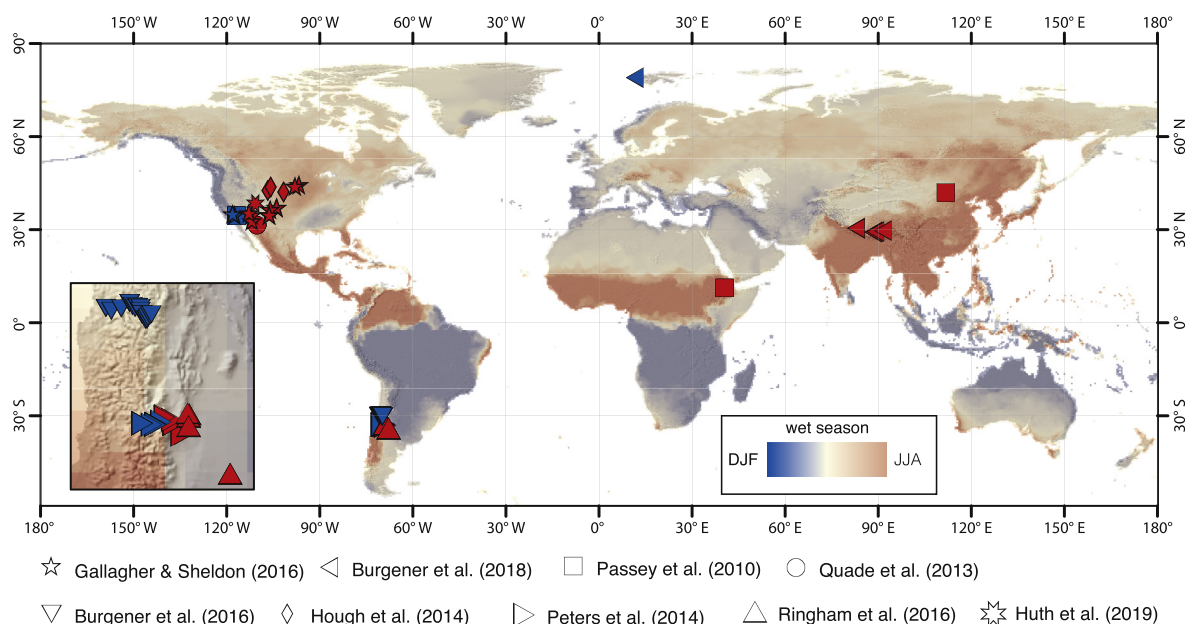


Fig. 1. Map highlighting precipitation seasonality and the locations of previously published studies considered in this review. Geometric shapes correspond to distinct studies and red versus blue color indicates summer or winter, respectively, as the primary season of precipitation. The precipitation seasonality image was created using 0.5° Global Precipitation Climatology Centre (GPCC) long-term mean monthly data (1981–2010) available from (<https://www.esrl.noaa.gov/index.html>). The sum of precipitation for DJF and JJA were subtracted from one another to highlight the seasonal extremes (note that the color switches: in the Northern hemisphere, blue indicates primarily winter (DJF) precipitation, while in the southern hemisphere red indicates primarily winter (JJA) precipitation). The resulting grid was overlain on a shaded relief image generated using ETOPO2 version 2 topographic data (<https://www.ngdc.noaa.gov/>). (For interpretation of the references to color in this figure legend, the reader is referred to the Web version of this article.)

or nearby weather stations. Table 1 lists the studies considered and the type of meteorological data. The methods used to identify and date Holocene carbonates vary by study: methods range from identifying and sampling young soils based on landscape position to radiocarbon dating of carbonate material. We do not include samples that the original studies identified as having precipitated in isotopic disequilibrium and/or as a statistical outlier (the cryogenic and outlier samples from Burgener et al. (2016) and Burgener et al. (2018)). From Huth et al. (2019), we only include sample D-025, which is the outermost and youngest carbonate rind studied in that paper.

3.2. Updating clumped isotope temperatures to modern standards

The Δ_{47} data in this compilation were acquired during a time of rapid methods development. We take several steps to update all data to be consistent with modern standards for number of replicate analysis and methods of calculation and standardization.

The first relatively recent advancement was the development of the 'absolute reference frame' or carbon dioxide equilibrium scale (CDES), created to enable interlaboratory comparison (Dennis et al., 2011). Many of the first analyses of modern soil carbonates were performed and published before the establishment of the CDES and are presented in the 'Ghosh' or 'Caltech' reference frame, which references sample data to measurements of carbon dioxide equilibrated at 1000 °C (e.g., Huntington et al., 2009); the Δ_{47} data in from Passey et al. (2010) are referenced this way. Some Δ_{47} values were retroactively projected into the CDES for publication (Quade et al., 2013; Peters et al., 2013; Hough et al., 2014). We include these data in our compilation but acknowledge that these Δ_{47} values might have additional, unquantifiable uncertainties.

Some early clumped isotope studies reported a single analysis for a given sample (an analysis is defined as a single acid digestion of carbonate and measurement of the resulting CO_2). Now it is

recognized that the small size of the Δ_{47} signal mandates more than a single analysis to produce robust data (Fernandez et al., 2017). Three replicates is typically considered a minimum to achieve the desired precision (Petersen et al., 2019; Spencer and Kim, 2015) and in some cases 5–6 replicate analyses are performed (~14 is considered a minimum for the LIDI analysis method, Müller et al. (2017)). We therefore conservatively remove Δ_{47} data for samples with only a single replicate from all studies (Fig. 2).

Recent work shows the importance of choosing correct ^{17}O correction parameters. Because they have the same atomic mass, ^{17}O -bearing CO_2 molecules interfere with the measurement of ^{13}C - and ^{18}O -bearing CO_2 molecules (e.g., Brand et al., 2010). The values used to correct for this interference affect the accuracy of Δ_{47} values (Daëron et al., 2016; Kelson et al., 2017; Schauer et al., 2016). Clumped isotope workers originally used the ^{17}O correction parameters recommended by Santrock et al. (1985) (e.g., Huntington et al., 2009); however, these values are based on terrestrial water and rock data for the quartz-water system and can produce spurious Δ_{47} values for carbonates (Daëron et al., 2016; Schauer et al., 2016). The ^{17}O values recommended by IUPAC (Brand et al., 2010) are more appropriate for carbonates and largely eliminate such errors; it is recommended that all future studies use those parameters (Daëron et al., 2016; Petersen et al., 2019; Schauer et al., 2016). Here, we recalculate $\delta^{13}\text{C}$, $\delta^{18}\text{O}$, and Δ_{47} values using the ^{17}O correction parameters recommended by IUPAC (Brand et al., 2010) where possible (Fig. 2).

To calculate temperatures from Δ_{47} values that were calculated with the IUPAC parameters, an empirical calibration constructed using measurements made with IUPAC parameters should be used. In most cases, this requires the use of a T- Δ_{47} calibration that differs from that used in the original publication of the Δ_{47} data. Most recent empirical calibrations are converging on a similar Δ_{47} -temperature sensitivity of approximately 0.04‰/°C, but some discrepancies still remain among labs, particularly in intercept

Table 1
Studies included, meteoric and soil texture data sources, data quality.

Study	Meteoric Data Source	Soil Texture Data Source	Samples with >1 replicate	Updated with IUPAC ^{17}O parameters?	Soil Texture ^a	Primary Season of Precipitation ^b
Passey et al. (2010)	Soil temperatures in Table S3 of paper, monthly mean air temperatures from local weather stations in Table S1 of paper	Descriptions of soils in supplement of original publication	9 of 28	no	fine/ medium/ coarse	summer/ winter
Quade et al. (2013)	Soil and air temperature from Fig. 2d of original paper	Not available	5 of 52	no	coarse	summer
Peters et al. (2013)	Soil temperature from Fig. 5 in original paper (only for select locales). Air temperature from local weather stations, extrapolated by elevation.	Field notes, photographs of soil pits, personal communication with authors	33 of 34	no	medium/ coarse/very coarse	summer/ winter
Hough et al. (2014)	Soil and air temperature from nearby SCAN sites. Used elevation-temperature relationship from Fig. 3 of paper.	Not available for sample matrix	8 of 14	yes	—	summer
Burgener et al. (2016)	Soil and air temperature measured in situ for some sites, extrapolated by elevation for others. Data from supplemental tables in paper.	Field notes, photographs of soil pits, personal communication with authors	36 of 36	yes	coarse/very coarse	winter
Ringham et al. (2016)	Soil and air temperature measured in situ for some sites, extrapolated by elevation for others. Data from supplemental tables in paper.	Field notes, photographs of soil pits, personal communication with authors	22 of 24	yes	medium/ coarse/very coarse	summer
Gallagher and Sheldon (2016)	Air temperature normals from nearby NCDC weather stations, provided in paper.	From NRCS soil series descriptions from sites, provided by T.G.	11 of 11	yes	fine/ medium/ coarse	summer/ winter
Burgener et al. (2018)	Air temperature from original paper Table 2 (local weather station data)	Categorized by texture in original publication	9 of 9	yes	medium	summer/ winter
Huth et al. (2019)	Air temperature from local weather station data (Teasdale, UT, GHEN station USC00428600)	Communication with T.H., photographs of soil trench, and soil texture notes	1 of 1	yes	coarse	summer

^a - Soil texture for individual samples is given in Table S1.

^b - Primary season of precipitation for individual samples is given in Table S1.

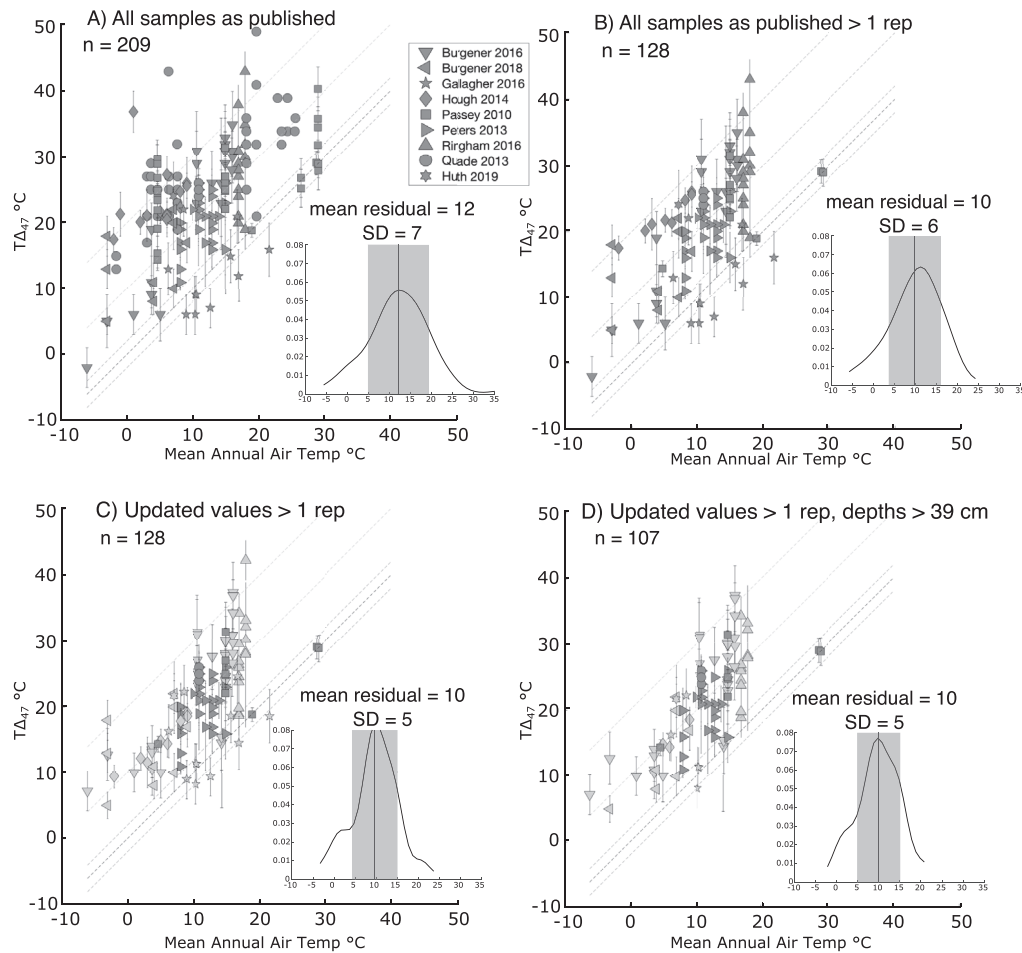


Fig. 2. Clumped isotope temperature vs mean annual air temperature for Holocene soil carbonate samples included in this work. In all panels, the dark gray dashed line is 1:1 line and light gray dashed lines are ± 2 , ± 10 , and ± 20 °C. Subplots are kernel density estimates of the residual between MAAT and $T\Delta_{47}$, with mean residual (± 1 S.D.) plotted as gray band. a) All samples as published in original work. b) Only samples that have more than a single Δ_{47} replicate analysis, with $T\Delta_{47}$ values as published in original studies. c) As in B, but dark gray samples indicate $T\Delta_{47}$ values have been recalculated to reflect modern standards as described in Section 2.2. Dark gray samples are not recalculated (lacked necessary data but are still included as discussed in Section 4.1). d) Recalculated $T\Delta_{47}$ data from samples >39 cm in depth.

(Bonifacie et al., 2017; Kele et al., 2015; Kelson et al., 2017; Levitt et al., 2018; Peral et al., 2018; Petersen et al., 2019). Thus, for each dataset, we use a $T\Delta_{47}$ calibration that was produced in the same laboratory as the soil carbonate data and that has been calculated with the IUPAC parameters (Table S3). These calibrations were reported in Supplementary Table 5 of Petersen et al. (2019) (Table S3). In all cases, we use an acid fractionation factor (AFF, Δ^*_{25-90}) of 0.088‰ to project samples reacted at 90 °C into the 25 °C reference frame, and an AFF of 0.072‰ to project samples reacted at 75 °C into the 25 °C reference frame (Δ^*_{25-75}), based on AFFs recalculated from 4 studies using IUPAC parameters (Petersen et al., 2019).

Error in the Δ_{47} values is reported as the standard error of the mean (S.E.) of replicate analyses of each carbonate sample (S.E. is defined as the standard deviation (S.D.) divided by the square root of the number of replicates). To calculate S.E., we employed whichever is larger: the long-term S.D. of a carbonate standard (carbonate standard information is listed in footnote of Table S1) or the S.D. of the replicate analyses. Where relevant, the oxygen isotopic composition of the soil water from which the soil carbonate grew ($\delta^{18}O_{sw}$) is recalculated using the IUPAC-recalculated $T\Delta_{47}$ values and the fractionation factor from Kim & O'Neil (1997). This choice in calcite-water fractionation factor (Kim and O'Neil, 1997) is smaller than other 'equilibrium' factors in the literature (e.g.,

Coplen, 2007), a choice that could bias the results to relatively higher calculated $\delta^{18}O_{sw}$ (values that are more similar to $\delta^{18}O$ of summer rain for samples in this study with the exception of the carbonates from Tibet in Burgener et al. (2018), Table S1).

3.3. Compiling environmental data

Previous studies of Holocene soil carbonates placed isotopic data in context of various environmental parameters. To consider the data altogether, we standardize the following environmental parameters: temperature, precipitation, $\delta^{18}O$ of rainfall, soil texture, and vegetation cover. These parameters are chosen based on practicality, availability, and their potential to be constrained in paleoenvironments.

Each sample was assigned a mean annual air temperature (MAAT) and mean warm season temperature (MWST, defined as the mean temperature of the warmest three months, which is either JJA or DJF in all places except the tropics, where it is MJJ). We use the air temperature data that is consistent with what was used in the original publications, which come from a variety of sources (Table 1). For some sites, carbonate samples were collected from soil pits with *in-situ* weather monitoring stations (Burgener et al., 2016; Peters et al., 2013; Ringham et al., 2016). For other sites,

temperature data come from weather stations at a similar elevation that are within a few kilometers of the sample collection site (Table 1). In some cases, temperatures were extrapolated between elevations to estimate a more accurate temperature at the given sample site. Each of these temperature sources has associated uncertainties that are difficult to quantify. Using meteorological data from non-*in-situ* sources might not be representative of the exact conditions of the sampled soil. Both meteorological and *in-situ* records are relatively short (ranging from 1 to 3 years for *in-situ* data to decades for meteorological stations) and thus may not be representative of soil conditions over hundreds to thousands of years over which the analyzed soil carbonates likely formed. We use air temperature to compare to Δ_{47} data because air temperature is generally the parameter of interest for paleoclimate reconstructions, and because direct observations of local soil temperature were not available for all samples.

For an initial and relatively simple characterization of precipitation regime, we assigned the primary season of precipitation to each sample based on examining local weather station records (defined as the three consecutive months, JJA vs. DJF, whichever has higher proportion of annual precipitation). The $\delta^{18}\text{O}$ value of annual precipitation (weighted by monthly precipitation, $\delta^{18}\text{O}_{\text{ann}}$) at each sample location was estimated using the Oxygen Isotopes in Precipitation Calculator (OIPC) (Bowen and Revenaugh, 2003), which is an algorithm that interpolates between point measurements of $\delta^{18}\text{O}$ values of rainfall to produce global maps of $\delta^{18}\text{O}$ values. The OIPC values may suffer in accuracy especially at high elevations and locations where measurements are sparse; nevertheless, we use these values because not all localities in our global dataset have measurements of local $\delta^{18}\text{O}$ values, and the local measurements that exist are from a variety of water sources (rain, snow, rivers, and lakes, not seasonally distributed point measurements). The uniformity of the OIPC calculator facilitates global comparisons of $\delta^{18}\text{O}$ values. Furthermore, it is analogous to comparing proxy-point data to regional output from isotope-enabled global circulation models of paleoclimate. To assess a seasonal bias in $\delta^{18}\text{O}_c$ relative to $\delta^{18}\text{O}$ from OIPC, we normalize the residual between $\delta^{18}\text{O}_c$ and mean annual from OIPC ($\delta^{18}\text{O}_{\text{ann}}$) (i.e., normalized residual = $(\delta^{18}\text{O}_{\text{sw}} - \delta^{18}\text{O}_{\text{ann}})/(\delta^{18}\text{O}_{\text{max}} - \delta^{18}\text{O}_{\text{ann}})$ where $\delta^{18}\text{O}_{\text{max}}$ is $\delta^{18}\text{O}_{\text{summer}}$ in all cases except for the samples from Tibet where it is $\delta^{18}\text{O}_{\text{winter}}$).

Vegetative cover at each location was determined using the MODIS landcover dataset (Friedl et al., 2010), which uses an algorithm to classify satellite into land cover types at 500-m resolution. Various algorithms exist that differ in how to categorize vegetative cover types for the sites examined, but the schemes that we examined all agreed in their classification of the barren/non-vegetated sites. Thus, we simplify the land cover classification and describe our sites as vegetated vs. non-vegetated. The sites that are categorized as 'non-vegetated' do have sparse vegetation but that term is used for consistency with the MODIS classification. This simplification into two land cover categories allows us to avoid making assumptions about the stability of the type of vegetation cover through the Holocene, like the proportion C3/C4 plants at a given sampling site (Ringham et al., 2016), and also circumvents the need to re-classify sites that are classified as 'urban' or 'cropland' — categories that are not pertinent to the carbonate that had been forming in soils before human occupation. Our two-category classification scheme is also consistent with a compilation of air and soil temperature data that show little difference in radiative heating amongst vegetation categories (Burgener et al., 2019). Although vegetative cover cannot be directly measured in paleosols, it might be inferred from paleosol morphology including root traces, paleosol organic carbon content, or local fossil records.

Soil texture of the matrix surrounding each sample was evaluated from descriptions in supplementary material, photographs of

the soil pits, field notes, and personal communication with authors (Table 1). Quantitative soil texture data such as hydraulic capacity, percent clay content, etc., does not exist. The soil texture categories in Table 1 are thus generally based on percent gravel and presence of sand, since that is straightforward to estimate from photographs. Each sample is assigned a soil texture category, where 'fine' indicates clay/silt, 'medium' indicates silt loam/sand (can contain minor gravels, as is the case for pendant samples), 'coarse' indicates matrix-supported gravels (gravels of about 50% or more of matrix, identified visually from pictures or in descriptions), and 'very coarse' indicates clast-supported gravels, following the classification scheme of Burgener et al. (2018). In the case of carbonate pendants, the soil texture refers to the average matrix grain size, not the size of the clast on which the carbonate pendants formed. Quantitative or semi-quantitative soil texture estimates can be made for paleosols at the outcrop.

4. Results

4.1. Updated Δ_{47} values

Of the 209 published Δ_{47} values from Holocene/recent soil carbonates, a total of 128 samples have >1 replicate analysis (study-specific information in Table 1). The data necessary to recalculate Δ_{47} values with updated ^{17}O parameters were available from supplementary data or personal communication with authors of the following studies: Burgener et al. (2016), Ringham et al. (2016), Hough et al. (2014), Gallagher and Sheldon (2016), and Huth et al. (2019) (Table 1). The Δ_{47} values of the samples in Burgener et al. (2018) were initially published using the updated Brand et al. (2010) parameters, so no re-calculation was needed. We were not able to recalculate the Δ_{47} values from Passey et al. (2010), Quade et al. (2013), or Peters et al. (2013). The data from these studies are included despite not being recalculated because they were generated at Caltech, and due to the isotopic composition of the reference gases used in that laboratory, the data likely do not have significant systematic errors from the use of the original Santrock et al. (1985) parameters (Bonifacie et al., 2017; Schauer et al., 2016).

As predicted by Daëron et al. (2016) and Schauer et al. (2016), the magnitude and direction of change in Δ_{47} due to using Brand et al. (2010) parameters depends on the isotopic composition of the natural sample and of the standards used by each laboratory and each analysis session (Fig. S1). The largest observed changes in final calculated temperature (Δ_{47}) were in samples from Burgener et al. (2016) (up to 11 °C change), Hough et al. (2014) (up to 9 °C change), and Ringham et al. (2016) (up to 8 °C change) (Supplemental Text S1).

4.2. Carbonate sample locations, carbonate types, and soil texture

The 128 samples that have more than one replicate are biased both in the geographic location and type of Holocene soil carbonates. Most soil carbonates were collected from North and South America, with only seven sample collection sites from Asia, three from Africa, and one from the Arctic (Svalbard). Most of the soil carbonates in this compilation are carbonate rinds (pendants) that form on the underside of large clasts. Only a handful of the samples are carbonate nodules (all 11 samples from Gallagher and Sheldon (2016); the Inner Mongolia and California samples from Passey et al. (2010); and the NAC sample from Ringham et al. (2016)).

The MWST, MAAT, primary season of precipitation, and $\delta^{18}\text{O}$ values of precipitation ($\delta^{18}\text{O}_{\text{MWS}}$ and $\delta^{18}\text{O}_{\text{ann}}$) for each location can also be found in Table S1. Quade et al. (2013) reported hottest month mean temperature for their locations, so that value is used

instead of MWST. Climate reanalysis data show that warmest month mean temperature and MWST only differ by approximately 2 °C at midlatitudes (the difference ranges from 1 to 5 °C globally, Fig. S5).

Comparison between $T\Delta_{47}$ and ambient air temperatures suggests significant variability in the seasonal timing of carbonate formation (Fig. 2). Most samples exhibit a warm-season bias, with $T\Delta_{47}$ values that are larger than MAAT: the mean exceedance from MAAT is 10 °C. The mean exceedance from MWST is 2 °C (Table 2), an amount of exceedance that would be indistinguishable given typical $T\Delta_{47}$ uncertainty of ± 2 –3 °C. The difference between $T\Delta_{47}$ values and MAAT ranges from -4 to 24 °C, a large range that suggests that the annual timing of carbonate formation varies. We find that calculated $\delta^{18}O_{sw}$ has no apparent seasonal bias relative to the $\delta^{18}O$ of rainfall in 49 of the 107 samples considered at depths >39 cm.

5. Discussion

In the following discussion, we show that updating Δ_{47} and $T\Delta_{47}$ values to modern standards removes the hottest $T\Delta_{47}$ estimates (Fig. 2). The updated data confirm that most soil carbonates record a temperature that is biased towards the warm season, but with variability. Some of the variability in apparent seasonal bias can be explained by depth below ground surface, soil texture, season of precipitation, and presence of vegetation. In some soil carbonates examined, the seasonal bias is observed in both $T\Delta_{47}$ and $\delta^{18}O_{sw}$. We suggest that environmental constraints can be leveraged in the geologic record to improve interpretations of the stable isotope composition of soil carbonates.

5.1. Updating Δ_{47} values removes the hottest $T\Delta_{47}$ values

Recalculating Δ_{47} values with updated ^{17}O correction parameters and corresponding temperature calibrations and culling data based on lack of replication might be expected to reduce variability in the residual between $T\Delta_{47}$ and mean annual air temperature. Removing samples with only one replicate analysis results in the most significant reduction in the residual variability, reducing the mean residual from mean annual temperatures ($T\Delta_{47} - MAAT$) from 12.0 to 9.6 °C and reducing the standard deviation of that residual from 7.3 to 6.2 °C (Fig. 2). This decrease in the mean residual and its variance comes from the removal of 43 single-analysis samples with $T\Delta_{47}$ that exceeded MAAT by > 10 °C, 16 of which exceeded MAAT by > 20 °C (most of which are from the earliest two studies, Passey et al. (2010) and Quade et al. (2013), and are from depths ranging from 10 to 280 cm) (Table 1 and Fig. 2).

These extremely high $T\Delta_{47}$ values were previously explained by local radiative heating (including carbonates from depths > 39 cm) (Passey et al., 2010; Quade et al., 2013). It is not possible to determine whether the high temperatures of these un-replicated,

relatively deep samples would change if replicated. However, of the remaining data, few $T\Delta_{47}$ values are hotter than mean summer air temperatures. Radiative heating likely affects shallow samples in extremely arid and bare localities, but our reanalysis suggests that $T\Delta_{47}$ values that are significantly hotter than MWST at depth in the soil column are atypical. Direct measurements of soil temperatures also indicate that radiative heating is only significant in certain environments: a comparison of soil and air temperatures from the Soil Climate Analysis Network (SCAN) suggests that soil temperatures only exceed summer air temperatures by 5 °C at shallow depths (<20 cm) in extremely arid conditions (MAP 0–30 cm/year) (Burgener et al., 2019; Gallagher et al., 2019). On average, soil temperatures at depths >20 cm do not exceed surface temperature by more than 3 °C in all land cover types (Burgener et al., 2019). This observation is consistent with other direct field measurements of ground temperatures that exceed air temperatures by < 4 °C (Bartlett et al., 2006; Breshers et al., 1998; Cermak et al., 2017; Passey et al., 2010). In summary, these data suggest that corrections for radiative heating should only be required to interpret the $T\Delta_{47}$ values of paleosol carbonates in arid environments with bare soils, which only occur today where MAP is < 30 cm/year (Gallagher et al., 2019), and/or for near-surface carbonates.

For samples with >1 replicate, the step of recalculating the Δ_{47} values using IUPAC ^{17}O parameters results in changes in $T\Delta_{47}$ of up to 11 °C. The magnitude and direction of change varies on a sample-basis (Supplementary Text S1, Fig. 2B and C). The reprocessed values of Δ_{47} from some studies do not change significantly. $T\Delta_{47}$ values from Gallagher et al. change by 1–2 °C; recalculation does not change the authors' main conclusions that soil carbonate formation temperatures can agree with mean annual air temperatures, especially in environments that lack excessively dry summers. The $T\Delta_{47}$ value of the sample from Huth et al. (2019) changes by < 1 °C, upholding their interpretation of a summertime-biased carbonate formation. The recalculation of the Ringham et al. (2016) samples does not significantly change the findings of that study. Two samples (NAC-85 and NAC-100) decrease in $T\Delta_{47}$ by 5 and 4 °C, respectively; all other samples decrease in $T\Delta_{47}$ by 1–2.5 °C. These authors did not explicitly determine a timing of carbonate formation, but examination of their meteorological data suggests that these $T\Delta_{47}$ values agree with or slightly underestimate midsummer soil temperatures, and the soil pit averages are within 1–2 °C of mean summer air temperature. One exception exists: CAN01 is 5 °C hotter than mean summer air temperature but agrees with summer soil temperature, which could be explained by local radiative heating, especially given that this soil pit has the highest percent of bare soil of the sites in this study. The primary findings of this study regarding depth-distributions of $T\Delta_{47}$ values remain unchanged (see discussion below), as does the apparent discrepancy between these samples and nearby samples analyzed by Peters et al. (2013).

However, some of the changes in $T\Delta_{47}$ are large enough to

Table 2
Seasonal Bias of Clumped Isotope Temperature and $\delta^{18}O$, by sample category.

	fine-grained	medium-grained	coarse-grained	very coarse-grained	winter	summer	summer (no fg)	vegetated	non-vegetated
num samples in group	4	18	29	22	43	44	39	77	51
Mean residuals from MAAT ($T\Delta_{47}$ -MAAT, in °C)									
Mean residuals	-0.3	7.6	10.6	11.0	11.1	8.2	9.1	8.3	11.7
S.D.	1.4	4.8	4.0	5.7	5.0	5.0	4.5	5.6	4.3
Mean residuals from MWST ($T\Delta_{47}$ -MWST, in °C)									
Mean residuals	-9.2	0.7	3.3	4.7	5.5	-0.1	0.9	0.0	5.8
S.D.	4.5	5.0	4.1	6.5	4.9	5.2	4.4	6.0	4.9
Mean residual from $\delta^{18}O_{ann}$ ($\delta^{18}O_{gw} - \delta^{18}O_{ann}$, in ‰)									
Mean residuals	-1.7	0.8	1.5	1.4	0.2	1.9	2.4	2.6	0.8
S.D.	2.9	2.6	3.4	3.2	2.7	3.5	3.4	3.8	2.9

require a re-evaluation of the originally published conclusions about timing of carbonate formation. First, recalculation of the data from Hough et al. (2014) results in a reduction in $T\Delta_{47}$ values of 6–9 °C. This change results in $T\Delta_{47}$ values that agree with mean warm season air temperatures rather than hotter than even the hottest month (July) air temperatures as originally described for all samples. Large changes in $T\Delta_{47}$ are also observed in select samples from Burgener et al. (2016). The recalculated $T\Delta_{47}$ value from the lowest elevation sample (Elq13-400-70) is 11 °C lower than as published (recalculated value of 15 °C vs. published value of 26 °C). This recalculated $T\Delta_{47}$ suggests that the sample formed at temperatures that are cooler than mean annual soil temperature (the original interpretation was that the $T\Delta_{47}$ was between mean summer and mean annual temperatures). The recalculated $T\Delta_{47}$ is consistent with field observations that the soil pit was still moist at the time of field work (mid-summer) where all other soil pits were dry. Changes in $T\Delta_{47}$ also occur at samples from the elevation range of 3200–4500 m. This group of samples was originally interpreted as agreeing best with mean annual soil temperature, and now appear to be between mean annual and summer soil temperatures. This reduces the difference in seasonal bias between samples above and below 3200 m that the authors originally observed and attributed to the local elevation of the snow line. There may still be a subtle shift in timing and mechanism of soil carbonate formation related to the presence or absence of snowpack, but the data now suggest a more uniform summer bias across all elevations in central Chile.

While the recalculated $T\Delta_{47}$ values change interpretations for select samples, overall the recalculation for the global dataset does not significantly change the mean or variance of the observed residual from MAAT (note that removing single analyses does change the mean, as described above). The as published and recalculated $T\Delta_{47}$ values for replicated samples are both characterized by a residual from mean annual air temperature ($T\Delta_{47}$ minus MAAT) of 10 °C (S.D. = 5–6 °C) (Fig. 2). Even with updated Δ_{47} values, the variation in observed seasonal bias is large compared to the ~2 °C precision usually desired to reconstruct paleoclimate conditions, making the interpretation of $T\Delta_{47}$ of paleosol carbonates challenging. In the following sections, we explore the extent to which variance in the relationship between air temperature (MAAT and MWST) and the observed $T\Delta_{47}$ values can be explained by sample depth, soil texture, seasonality of precipitation, and land cover.

5.2. No systematic relationship between $T\Delta_{47}$ and depth in the soil

Because soil temperatures vary with depth and time as fluctuations in temperature at the surface propagate downward, it was predicted that summertime formation of soil carbonates would result in carbonate temperature increasing toward the surface in the upper 100 cm of soil. Such an increase in carbonate temperature toward the surface was observed by Quade et al. (2013) in one of the first studies of Δ_{47} of soil carbonates. However, subsequent workers found that $T\Delta_{47}$ does not vary systematically with depth within a single soil profile (Burgener et al., 2016; Peters et al., 2013; Ringham et al., 2016). We re-evaluate the variation of $T\Delta_{47}$ with depth in the updated compilation.

The compiled $T\Delta_{47}$ depth profiles of soil pits includes the majority of data from Peters et al. (2013), Burgener et al. (2016) and Ringham et al. (2016), as well as the Huachuca pit from Quade et al. (2013). The Quade et al. (2013) data that showed systematic warming of carbonate formation temperatures near the surface were based on un-replicated Δ_{47} analyses. Within the 15 soil pits with replicated data, $T\Delta_{47}$ does not vary systematically with depth (from 0 to 150 cm) within measurement error (Fig. 3, Fig. S2). 68 of the 75 individual carbonate samples in the updated compilation of

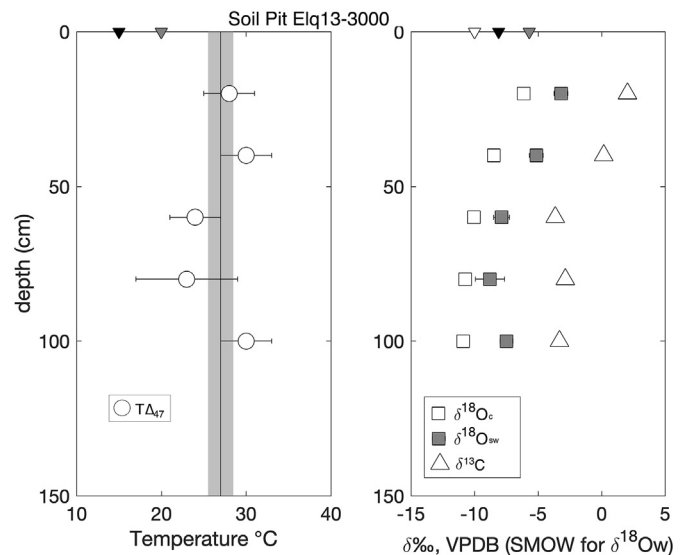


Fig. 3. Stable isotope depth profiles for soil pit Elq13-3000, located at 1300 m in elevation in the Elqui Valley, Chile (Burgener et al., 2016). Left panel: open circles are $T\Delta_{47}$ values at specific depths. Vertical gray band is soil pit mean $T\Delta_{47} \pm 1$ S.E. Black/gray triangles on top of plot are MAAT/MWST. Right panel: open squares are $\delta^{18}O_{sw}$, gray squares are calculated $\delta^{18}O_{ann}/\delta^{18}O_{HA}$ of rain from OIPC. Open triangles are $\delta^{13}C$.

depth profiles have a $T\Delta_{47}$ value that is within 1 S.E. of the mean temperature of the profile (Fig. S2). Only one shallow sample has a $T\Delta_{47}$ value that exceeds summer air temperatures by an amount that suggests radiative heating has affected shallow soil temperatures (CAN01-10, from Ringham et al., 2016, $T\Delta_{47} = 42 \pm 4$ °C vs. MWST = 25 °C). The observed uniform $T\Delta_{47}$ values within a soil column could result from the following end-member scenarios: 1) soil carbonate forms approximately simultaneously at all depths when temperature is uniform with depth in a soil, or 2) soil carbonate formation occurs at different times at different depths but result in the same growth temperature within measurement precision (usually ± 2 °C). To be valid, the scenario must be consistent with the available $\delta^{13}C$ and $\delta^{18}O$ values as well as the Δ_{47} data.

In the first scenario, the observed uniform $T\Delta_{47}$ values with depth are explained by soil carbonate forming at all depths simultaneously when soil temperatures are uniform. Such uniform temperatures at depth in a soil column can occur following rain events as percolating rainwater moves downward (as shown by meteorological and in-situ data collected by Ringham et al., 2016). A pulse of soil moisture could dilute the organic carbon content and promote carbonate precipitation (Marion et al., 2008). However, the $\delta^{13}C$ and $\delta^{18}O$ data are not necessarily consistent with soil carbonate formation following rain/wetting events. $\delta^{13}C$ values increase toward the surface and generally resemble the prediction for $\delta^{13}C$ with depth that is calculated from a steady state CO_2 production-diffusion model (described in Quade et al. (1989); Cerling (1984)) (this is especially true for the pits Elq13–1300, A Peters, Elq13-2700, D2 Peters, DL01 Ringham, CA Passey, see Fig. S2). This systematic $\delta^{13}C$ decrease with depth might suggest that soil carbonate is forming under conditions of time-constant or time-averaged soil respiration. However, soil respiration can spike following wetting events (Borken et al., 2003; Bowling et al., 2011; Lee et al., 2004; Liu et al., 2002; Tang and Baldocchi, 2005) – so perhaps the $\delta^{13}C$ data are inconsistent with carbonate formation after storms when soil CO_2 is changing rapidly. Furthermore, we might expect such percolation of rainwater to remove or dampen the near-surface evaporative enrichment in ^{18}O , but most soil pit

data show an increase in calculated $\delta^{18}\text{O}_{\text{SW}}$ values toward the surface (Fig. 3, Fig. S2).

Given this isotopic evidence, it remains equally possible that soil carbonates form at different times at different depths but result in near-uniform $\text{T}\Delta_{47}$ profiles. This might occur because near-surface soil carbonates are more vulnerable to daily fluctuations in temperature/precipitation and form during drying after small rain events throughout the year, while deeper carbonate only form after large rain events and/or during seasonal drying (McFadden and Tinsley, 1985; Retallack, 2005; Ringham et al., 2016). This process of soil carbonate formation implies that near-surface carbonates (0–39 cm in depth, where 40 cm is maximum depth affected by daily temperature fluctuations) record an isotopic signal that is more variable and more challenging to interpret than carbonates at depths >40 cm (Ringham et al., 2016; Quade et al., 2013). This difference in timing of formation, even within a single soil pit, could explain some of the variance in soil carbonate $\delta^{13}\text{C}$, $\delta^{18}\text{O}$ and Δ_{47} data.

The compiled dataset suggests that $\text{T}\Delta_{47}$ is uniform with depth in the studied environments, but further research is necessary to explain why. Given this outstanding question, and the documented variability in $\delta^{13}\text{C}$ and $\delta^{18}\text{O}$ values, we maintain the longstanding recommendation that near-surface carbonate samples (approximately 0–40 cm in depth) should be avoided for use in paleoclimate reconstructions (Cerling and Quade, 1993; Quade et al., 2013, 2007). We simplify the remainder of the discussion by conservatively disregarding the samples collected from 0 to 39 cm in depth. Removing these near-surface samples from the compilation dataset results in a minor increase in the mean bias between soil carbonate $\text{T}\Delta_{47}$ and MAAT of 0.5 °C (from 9.6 to 10.1 °C, S.D. = 5) and reduces the S.D. from 5.4 to 5.0 °C (Fig. 2).

5.3. Soil texture and $\text{T}\Delta_{47}$ values

Soil texture is a parameter that could be directly measured in paleosols and may influence soil carbonate formation through changing soil hydrology. The grain size of a soil matrix is a primary control on its hydraulic properties (e.g., Carsel and Parrish, 1988;

Fredlund and Xing, 1994) so it has been suggested that grain size could influence the timing of soil carbonate formation (Burgener et al., 2018). Because fine-grained soils retain moisture better than coarse-grained soils, the timing of soil drying should differ with soil texture. The coefficient for CO_2 diffusion out of a soil column also depends on grain size, such that if all else is equal soil CO_2 concentrations will decrease more slowly in fine-grained soils (Bouma and Bryla, 2000; Suarez and Šimůnek, 1997). Thus, coarse-grained soils should dry and degas faster than fine-grained soils, which may cause soil carbonate in coarse-grained soils to form sooner after rain events. We examine the compiled dataset for patterns in $\text{T}\Delta_{47}$ that relate to soil texture.

The four samples that are fine-grained (silty clay) are statistically different from the other sample populations, but we note that this is a very small population size. The fine-grained samples have a mean $\text{T}\Delta_{47}$ – MAAT residual of -0.3 °C (S.D. = 1 °C) (Table 2), which is a statistically colder bias than the other texture categories (Table 3). Furthermore, a KS-test shows that the fine-grained sample group are unlikely to have come from the same continuous underlying distribution as the other sample types (Table 3) (Fig. 4). However, three of the four fine-grained samples are from a single study (Gallagher and Sheldon, 2016) and the fourth sample is from Ethiopia (Passey et al., 2010), where there is no seasonal range in temperature. Also, two fine-grained samples that formed at depths <39 cm (i.e., not discussed above) have $\text{T}\Delta_{47}$ values that are similar to summer air temperatures (Kranzburg and Clamo samples from Gallagher and Sheldon (2016)), suggesting that fine-grained soils do not always result in reduced clumped isotope temperatures. These data hint that soil carbonates in clay-rich substrates are more likely to have a growth temperature that is closer to MAAT than those from coarse soils, but additional data on soil carbonates from fine-grained soils are needed to rigorously test this hypothesis.

$\text{T}\Delta_{47}$ data from soil carbonates in the other soil-texture categories (medium, coarse, and very coarse-grained), also suggest that soil texture can explain some of the variability in seasonal bias. Carbonates from the medium, coarse, and very-coarse grained soils

Table 3
Results on Statistical Comparisons (KS test and *t*-test) Between Sample Populations.

	fine vs. medium grained	fine vs. coarse grained	fine vs. very coarse grained	medium vs. coarse grained	medium vs. very coarse grained	coarse vs. very coarse grained	winter vs. summer precip	winter vs. summer precip, without fg	vegetated vs. non vegetated
<i>KS test results - comparisons of $\text{T}\Delta_{47}$-MAAT^a</i>									
h	1	1	1	1	0	0	0	0	1
p	0.0017	7.70E-04	5.73E-04	0.0247	0.4648	0.3228	0.0696	0.2826	0.0139
ks-stat	0.9444	0.9655	1	0.4253	0.2576	0.2586	0.2696	0.2105	0.2776
<i>t-test results - comparisons of $\text{T}\Delta_{47}$-MAAT for each population^b</i>									
h	1	1	1	1	1	0	1	1	1
p	5.40E-03	1.12E-05	7.80E-04	2.27E-02	4.97E-02	8.07E-01	0.0073	0.0466	3.23E-04
difference in means \pm 95% CI (°C)	7.8 \pm 5.2	10.9 \pm 4.3	11.3 \pm 6.0	3.1 \pm 2.6	3.4 \pm 3.4	0.3 \pm 2.8	2.9 \pm 2.1	2.0 \pm 2.0	3.4 \pm 1.8
<i>KS test results - comparisons of $\text{d}18\text{O}_{\text{gw}}-\text{d}18\text{O}_{\text{ann}}^{\text{a}}$</i>									
h	0	0	0	0	0	0	1	1	1
p	0.1351	0.1661	1.44E-01	0.2217	0.8639	0.0742	0.0414	0.0223	0.0168
ks-stat	0.5833	0.5432	0.5682	0.3008	0.1818	0.348	0.2896	0.3192	0.2722
<i>t-test results - comparisons of $\text{d}18\text{O}_{\text{gw}}-\text{d}18\text{O}_{\text{ann}}^{\text{b}}$</i>									
h	0	0	0	0	0	0	1	1	1
p	1.14E-01	8.80E-02	8.95E-02	4.21E-01	5.36E-01	8.42E-01	0.0086	0.0016	0.0037
difference in means \pm 95% CI (‰)	NA	NA	NA	NA	NA	NA	1.8 \pm 1.3	2.2 \pm 1.3	1.8 \pm 1.2

^a Tests the null hypothesis that the residual ($\text{T}\Delta_{47}$ -MAAT) data are from the same continuous distribution, using the two-sample Kolmogorov-Smirnov test. If $h = 1$, it rejects the null hypothesis at the 5% significance level (different distributions, in bold).

^b Tests the null hypothesis that the residual ($\text{T}\Delta_{47}$ -MAAT) data are from the populations with the same mean. If $h = 1$, it rejects the null hypothesis at the 5% significance level (different means, in bold).

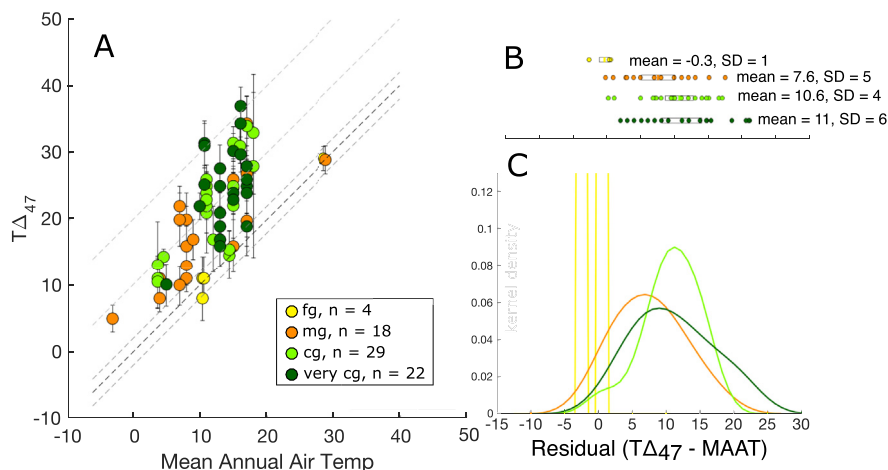


Fig. 4. Soil texture and apparent seasonal bias of $T\Delta_{47}$ of soil carbonates. Symbol color indicates soil texture (fine, medium, coarse, and very coarse-grained matrix). A) Clumped isotope temperature vs mean annual air temperature for carbonates from compiled dataset. Dark gray dashed line is 1:1 line, light gray dashed lines are ± 2 , $+10$, and $+20$ °C. B) Residual between $T\Delta_{47}$ and MAAT for each carbonate sample, binned by texture. C) Kernel density of the residual. The small population size for the fine-grained group ($n = 4$) results in a spurious kernel density. (For interpretation of the references to color in this figure legend, the reader is referred to the Web version of this article.)

have mean seasonal biases that increase with coarseness in soil texture (mean bias 7.5, 10.7, and 11.0 °C, respectively) (Table 2) (Fig. 4). Although the carbonate samples from these groups likely came from the same continuous distribution (see KS test results in Table 3), the mean temperature of carbonate formation in medium-grained soils is significantly different from the mean in coarse- and very coarse-grained samples (t -test in Table 3) (Fig. 4). Nonetheless, the trend among texture categories and the significant difference between the means of fine, medium and very coarse textured soils suggests that coarser soils may be more likely to have a larger seasonal bias.

In summation, these limited data suggest that coarser soils are more likely to yield carbonates with a warm season bias compared to fine-grained soils. The difference in seasonal bias is less pronounced when comparing carbonates in adjacent categories from medium-to coarse-grained soils. One limitation of this current analysis is that we are qualitatively describing soil texture based on photographs and field notes; some of the coarse-grained soils might have clay in the matrix, which complicates our interpretations. Measurements of grain size distributions and quantifications of clay content are necessary to further address the role that soil texture plays in soil carbonate formation.

5.4. Timing of rainfall and $T\Delta_{47}$ values

One of the first studies of Δ_{47} of soil carbonates found a difference in the apparent timing of carbonate formation that corresponded with a difference in the annual timing of rainfall: soil carbonates in environments with winter rain had a higher $T\Delta_{47}$ relative to mean annual soil temperatures than soil carbonates from a summer rain environment (Peters et al., 2013). This work led to the hypothesis that the timing of rainfall is linked to the timing of soil drying, and thus linked to the timing of soil carbonate formation. Versions of the ‘soil drying’ framework include that soil carbonate formation should occur after the wettest season of the year (Gallagher and Sheldon, 2016; Peters et al., 2013), during seasonal warming in especially dry years (Breecker et al., 2009), or in the summer after infiltration/storm events (Huth et al., 2019). The annual timing of soil drying is related to annual timing of rain/snow, although factors like flashiness of precipitation, snowpack/melt, plant growth, and clay content will complicate that relationship. In addition to influencing the timing of soil drying, the

annual timing of seasonal precipitation might influence soil temperatures: summertime rain might reduce maximum soil temperatures through the higher heat capacity of soil and evaporative cooling (Seneviratne et al., 2010), and, speculatively, through increased vegetation cover (Gallagher et al., 2019; Geiger et al., 2009). Thus, given its hypothesized control on soil drying and soil temperatures, and the potential ability to estimate dominant precipitation regimes in geologic settings, we explore if the annual timing in rainfall influences soil carbonate $T\Delta_{47}$ in a systematic way.

We find a small but statistically significant difference in the apparent seasonality between samples formed in summer vs. winter precipitation environments. The mean residual between $T\Delta_{47}$ and MAAT for the winter rain/snow samples is 11.1 °C ($n = 43$, S.D. = 5 °C) (Table 2) (Fig. 5), a value that is consistent with a warm season bias at mid latitudes. The mean residual between $T\Delta_{47}$ and MAAT for the summer-rain samples is 8.2 °C ($n = 44$, S.D. = 5 °C) (Table 2) (Fig. 5), a value that is closer to MAAT and 1.8 °C less than that of the winter-rain/snow samples (95% CI in difference of means from a t -test, Table 3). The observed difference in mean residuals between summer and winter rain/snow samples exists even if the fine-grained samples with a statistically smaller $T\Delta_{47}$ -MAAT residual are removed from the sample set (samples come from populations with different means at 95% CI, Table 3).

While we observe that samples grown in summer rain environments have lower clumped isotope temperatures as a population, the mean residuals from MAAT overlap within 1 S.D. with the winter rain samples. Seasonal timing of rainfall does not appear to be the primary control on the apparent seasonal bias in clumped isotope temperatures; this result might provide evidence against the prevailing hypothesis that carbonates form during soil drying. We speculate that the total amount of precipitation, the amount and style of precipitation in each season, and snowpack (see Huth et al., 2019; Burgener et al., 2016) may be complicating and important factors.

5.5. Vegetation cover and $T\Delta_{47}$ values

Because plants change water, solute, and CO_2 content in soils, and provide shade, their presence and the timing of their activity has been predicted to influence the timing and temperature of soil carbonate formation (Gallagher et al., 2019; Meyer et al., 2014; Noy-Meir, 1973; Ringham et al., 2016; Young et al., 2009). No evidence

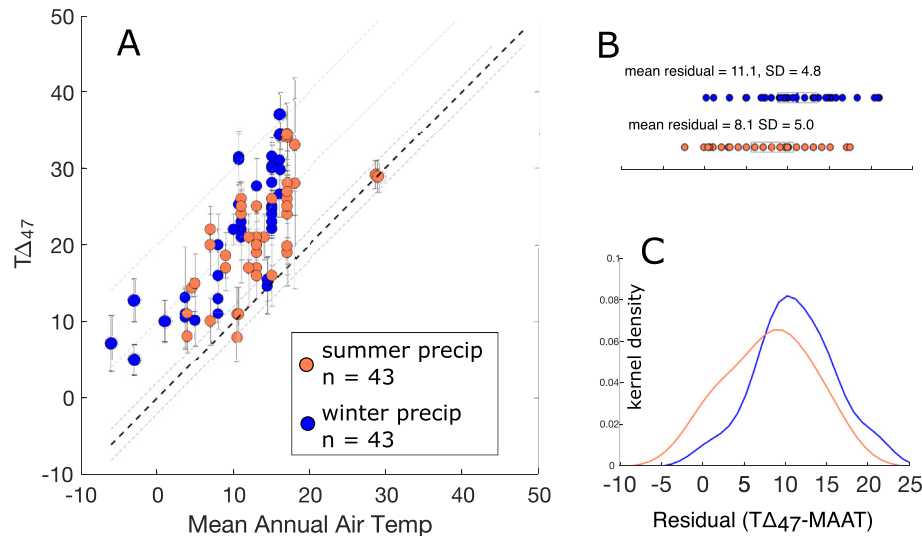


Fig. 5. Precipitation season and apparent seasonal bias of $T\Delta_{47}$ of soil carbonates. Blue symbol color indicates that the soil carbonate is from an environment with winter-dominated precipitation. Red symbol color indicates that the soil carbonate is from an environment with summer-dominated precipitation. A) Clumped isotope temperature vs mean annual air temperature for carbonates from compiled dataset. Dark gray dashed line is 1:1 line, light gray dashed lines are ± 2 , $+10$, and $+20$ °C. B) residual between $T\Delta_{47}$ and MAAT for each carbonate sample, binned by season of precipitation. C) Kernel density of the residual. (For interpretation of the references to color in this figure legend, the reader is referred to the Web version of this article.)

for significantly different $T\Delta_{47}$ values was found in soils that differed in the proportion of C3/C4 vegetation studied by (Ringham et al., 2016), a finding that does not change with the recalculated Δ_{47} values. We explore if the compiled $T\Delta_{47}$ values exhibit variation that is consistent with the presence or absence of vegetation; one could constrain paleo-vegetation with organic carbon content and/or plant fossils.

The mean residual between $T\Delta_{47}$ and MAAT for sites that are vegetated is statistically smaller than that of the non-vegetated sites (8 °C vs. 11 °C, different at 95% confidence interval with $p = e-4$ in a t -test) (Table 2, Table 3) (Fig. 6). The lower $T\Delta_{47}$ -MAAT residual for vegetated sites could be because plant activity promotes carbonate formation during the spring through rootwater uptake and changing soil CO_2 concentrations, even without the

benefit of long warm dry spells (Breecker et al., 2009; Meyer et al., 2014). The lower $T\Delta_{47}$ -MAAT residual could also be because vegetative shade might reduce radiative heating of ground temperatures in the summer (Cermak et al., 2017; Geiger et al., 2009; Passey, 2012). We prefer the former explanation because the depth profiles in this compilation show little evidence for radiative heating (see above) and other empirical evidence that soil temperatures at depths > 50 cm are not affected by radiative heating (Burgener et al., 2019).

5.6. Relationship between $\delta^{18}\text{O}$ values of carbonates and rainfall

Here we use the recalculated dataset to consider if $\delta^{18}\text{O}_{\text{sw}}$ values calculated from carbonates are biased toward a seasonal value of

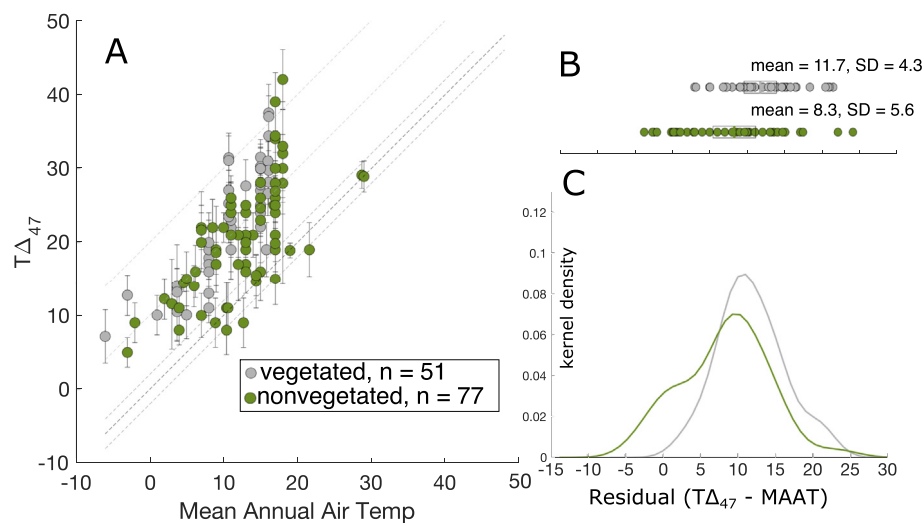


Fig. 6. Land cover and apparent seasonal bias of $T\Delta_{47}$ of soil carbonates. Symbol color indicates land cover (green is vegetated, gray is non-vegetated as determined by remotely sensed land cover algorithms of (Friedl et al., 2010)). A) Clumped isotope temperature vs mean annual air temperature for carbonates from compiled dataset. Dark gray dashed line is 1:1 line, light gray dashed lines are ± 2 , $+10$, and $+20$ °C. B) residual between $T\Delta_{47}$ and MAAT for each carbonate sample, binned by land cover. C) Kernel density of the residual. (For interpretation of the references to color in this figure legend, the reader is referred to the Web version of this article.)

rainfall $\delta^{18}\text{O}$ – which might be a logical prediction given apparent seasonal biases in $T\Delta_{47}$ (as proposed in Hough et al., 2014; Gallagher and Sheldon, 2016; and Huth et al., 2019). Overall, the compiled data show a significant positive correlation between $\delta^{18}\text{O}_{\text{sw}}$ and $\delta^{18}\text{O}$ values of weighted mean annual precipitation ($\delta^{18}\text{O}_{\text{ann}}$) (linear fit yields $r^2 = 0.528$, $p = 1.6e^{-15}$) (Fig. 7) – a relationship that might exist even if there is a seasonal bias in $\delta^{18}\text{O}_{\text{sw}}$. In comparison, the correlation between $\delta^{18}\text{O}_{\text{sw}}$ and $\delta^{18}\text{O}_{\text{summ}}$ yields a lower r^2 ($r^2 = 0.459$, $p = 5.94e^{-13}$). The correlation n between $\delta^{18}\text{O}_{\text{sw}}$ and $\delta^{18}\text{O}_{\text{ann}}$ is far from perfect, however, as $\delta^{18}\text{O}_{\text{sw}}$ differs from $\delta^{18}\text{O}_{\text{ann}}$ by up to 10‰. Just under half of the samples have a $\delta^{18}\text{O}_{\text{sw}}$ value that is closer to $\delta^{18}\text{O}$ of summer than to $\delta^{18}\text{O}_{\text{ann}}$ (49 of the 107 samples at depths > 39 cm) (Fig. 7 and Fig. S2), suggesting that seasonal biases can exist. Next we reconsider individual sample sets in order to explore the factors that promote deviation between $\delta^{18}\text{O}_{\text{sw}}$ and $\delta^{18}\text{O}_{\text{ann}}$, and if/when that deviation represents a seasonal bias.

In some cases, apparent negative deviations from $\delta^{18}\text{O}_{\text{ann}}$ values can be attributed to inaccuracies in the OIPC predicted values. First, a subset of the high-elevation samples from Peters et al. (samples from the ‘A’ pit and MODS07-07 and MODS07-10) have $\delta^{18}\text{O}_{\text{sw}}$ values (~13‰) that agree better with the $\delta^{18}\text{O}$ values measured in the Rio Mendoza and extrapolated by elevation (Hoke et al., 2009) (river water is ~11.3‰ while the OIPC predicts $\delta^{18}\text{O}_{\text{ann}}$ of ~10‰). Similarly, two samples from Ethiopia presented in Passey et al. (2010) (GONJQ-305-1 and GON07-4.701) have $\delta^{18}\text{O}_{\text{sw}}$ values of -2.3 and -0.3‰ that are more similar to local measurements of meteoric waters (average -0.2 ± 1.8 ‰ (Levin et al., 2009)) than

they are to the corresponding OIPC- $\delta^{18}\text{O}_{\text{ann}}$ values of +3.3 and +3.4‰. In these cases, when local meteoric waters are considered instead of $\delta^{18}\text{O}_{\text{ann}}$ from the OIPC prediction, we observe that these samples do not have an obvious seasonal bias in $\delta^{18}\text{O}_{\text{sw}}$. These inaccuracies in the OIPC in select locations might explain why some samples in our dataset that appear to have calculated $\delta^{18}\text{O}_{\text{sw}}$ values that are significantly lower than $\delta^{18}\text{O}_{\text{ann}}$ (Fig. 7).

A large relative enrichment in $^{18}\text{O}_{\text{sw}}$ is observed in samples of Ringham et al. (2016): sample values are 5–10‰ higher than $\delta^{18}\text{O}_{\text{ann}}$ ($\delta^{18}\text{O}_{\text{sw}}$ of 0–4.5‰, $\delta^{18}\text{O}_{\text{ann}}$ of -7.5 to -6.2‰, Table S1). Two of the carbonates recording large ^{18}O enrichments formed at depths less than 40 cm and could be partially explained by evaporation. However, the samples with anomalously high $\delta^{18}\text{O}_{\text{sw}}$ values are not from particularly arid environments compared to others in our study compilation (mean annual precipitation of about 220 mm), nor are they the samples with the highest $T\Delta_{47}$ values that might point to an enhanced seasonal bias in that location. It is notable that the soil carbonates with the highest $\delta^{18}\text{O}_c/\delta^{18}\text{O}_{\text{sw}}$ values are all pendants, while the nodular carbonates from the same study (from Nacunan) have $\delta^{18}\text{O}_{\text{sw}}$ values that are in good agreement of $\delta^{18}\text{O}_{\text{ann}}$ (within 1‰). This pattern does not always hold – there are many pendants that have $\delta^{18}\text{O}_{\text{sw}}$ values within 2‰ of $\delta^{18}\text{O}_{\text{ann}}$ (in Peters et al. (2013) and Burgener et al. (2016) datasets). However, this comparison points to a need to understand how various carbonate morphologies form and therefore what they may record.

Next, we reconsider select samples that were originally used to demonstrate a seasonal bias in $\delta^{18}\text{O}_{\text{sw}}$. Hough et al. (2014) originally showed agreement between $\delta^{18}\text{O}_{\text{sw}}$ and $\delta^{18}\text{O}$ values of summer

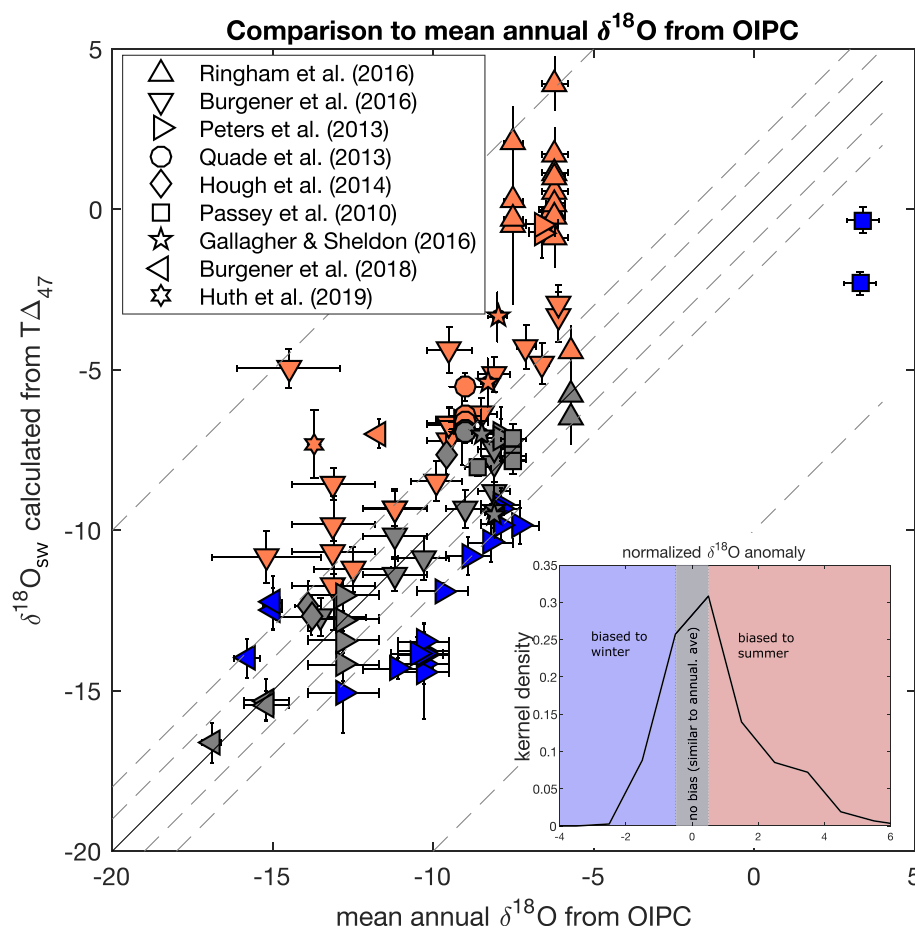


Fig. 7. Calculated $\delta^{18}\text{O}_{\text{sw}}$ and $\delta^{18}\text{O}$ values of rain water for soil carbonate samples.

rainfall in all of their sites in Nebraska and Wyoming, USA. However, the $\delta^{18}\text{O}_{\text{sw}}$ values that we recalculate are 1.4–2.0‰ lower than the originally reported values and change the original interpretation. The recalculated data suggest that only two of their samples have $\delta^{18}\text{O}_{\text{sw}}$ values that agree best with summer rain (WY11–C12 and WY11–C20), while two have values that are between the $\delta^{18}\text{O}$ values of summer rain and annual rain (NE11–C2 and NE11–C24), and the four remaining samples have $\delta^{18}\text{O}_{\text{sw}}$ values that are most similar to $\delta^{18}\text{O}$ values of annual rain. Thus the observed seasonal bias in $\delta^{18}\text{O}_{\text{sw}}$ does not always correspond with the observed summer bias in $\text{T}\Delta_{47}$ in all of the samples in Hough et al. (2014).

Similarly, Gallagher and Sheldon (2016) made the argument that $\delta^{18}\text{O}_{\text{sw}}$ best agrees with the $\delta^{18}\text{O}$ value of rain from the first month with no soil water storage (which was also the inferred month of carbonate formation). This inferred relationship holds true for the recalculated values from this study. Gallagher and Sheldon (2016) originally interpreted the Kranzburg and Clamo samples from South Dakota as having $\delta^{18}\text{O}_{\text{sw}}$ consistent with $\delta^{18}\text{O}$ of August and July. We calculate that the Kranzburg and Clamo samples from South Dakota have $\delta^{18}\text{O}_{\text{sw}}$ that is 2.9 and 4.4‰ higher than $\delta^{18}\text{O}_{\text{ann}}$, consistent with the originally inferred summer bias in $\delta^{18}\text{O}_{\text{c}}$. All other samples were originally interpreted as having $\delta^{18}\text{O}_{\text{sw}}$ consistent with $\delta^{18}\text{O}$ value of rainfall from either April or March, which is effectively similar to the $\delta^{18}\text{O}_{\text{ann}}$ values that they are compared against in this study (Fig. 7). Thus, of the samples from Gallagher and Sheldon (2016), two have $\delta^{18}\text{O}_{\text{c}}$ and $\text{T}\Delta_{47}$ values that are clearly summer-biased, while other samples $\delta^{18}\text{O}_{\text{sw}}$ values that are compatible with either a fall- or spring-season bias or an annual average.

In summary, $\delta^{18}\text{O}_{\text{sw}}$ values are not clearly biased toward seasonal $\delta^{18}\text{O}$ of rainfall in all environments. Within our dataset, we can find examples where an apparent summer bias is observed in both $\text{T}\Delta_{47}$ and in $\delta^{18}\text{O}_{\text{sw}}$ (e.g., two of the Hough et al., 2014 samples, the Peters et al., 2013 pit D samples). In most places, we observe an apparent summer bias in $\text{T}\Delta_{47}$ but no clear bias in $\delta^{18}\text{O}_{\text{sw}}$ values (Table S1); there is little correlation between normalized $\delta^{18}\text{O}_{\text{sw}}$ bias and temperature bias. A multitude of reasons could be invoked to explain why $\delta^{18}\text{O}_{\text{c}}$ values (and calculated $\delta^{18}\text{O}_{\text{sw}}$ values) are not consistently seasonally biased, even while $\text{T}\Delta_{47}$ values point to a seasonal bias in the timing of carbonate formation. First, $\delta^{18}\text{O}$ values of soil water might not vary sinusoidally with seasons even if $\delta^{18}\text{O}$ values of rainfall do. For example, seasonal variations in $\delta^{18}\text{O}$ values of rain could be dampened in soil as rainwater mixes with water stored in soil pores (Mathieu and Bariac, 1996). The rate at which rainwater percolates through the soil depends on rain intensity, depth in the soil, and soil texture. Also, evaporation will likely be depth- and texture-dependent, and could overprint all other soil-hydrology processes (Hsieh et al., 1998; Oerter and Amundson, 2016). The rate and amount of evaporation might depend on the gradient between soil and atmospheric relative humidity (Supplemental Fig. S7). We find that the mean residual between $\delta^{18}\text{O}_{\text{sw}}$ and $\delta^{18}\text{O}_{\text{ann}}$ values increases with increasing grain size (negative residual for fine-grained samples, increasingly positive for medium through very coarse-grained samples, perhaps due to increased evaporative enrichment or decreased water storage in coarse-grained soils) (Table 2, *t*-test results in Table 3). Also, the mean residual between $\delta^{18}\text{O}_{\text{sw}}$ and $\delta^{18}\text{O}_{\text{ann}}$ values is statistically larger for the samples in summer rain climates compared to those in winter rain climates (Table 2, Table 3). These results provide evidence for the idea that variations in $\delta^{18}\text{O}$ values of soil water (and thus $\delta^{18}\text{O}_{\text{c}}$ and $\delta^{18}\text{O}_{\text{sw}}$) are influenced by seasonality of rainfall and soil texture. However, these environmental factors can both increase and decrease $\delta^{18}\text{O}_{\text{sw}}$ compared to $\delta^{18}\text{O}$ of rainfall but sum to create $\delta^{18}\text{O}_{\text{sw}}$ that is apparently similar to $\delta^{18}\text{O}_{\text{ann}}$ in many soils (Fig. 7).

5.7. Outstanding conundrums and future directions for understanding $\text{T}\Delta_{47}$ of soil carbonates

While the environmental factors explored in this paper each explain a portion of the variation in $\text{T}\Delta_{47}$ biases, they are not precise predictors of the seasonal bias of soil carbonates: a $\sim 20^\circ\text{C}$ range in residual from MAAT exists within each category (Figs. 4, Figure 5, Fig. 6). Regional comparisons highlight existing conundrums: differences in $\text{T}\Delta_{47}$ occur even in environments that seem similar based on the parameters that we examined. For example, samples from Wyoming at elevations of about 2000 m have $\text{T}\Delta_{47}$ values that exceed MAAT by about 10°C (consistent with summer formation) (three carbonate pendant samples from Hough et al., 2014), while samples from New Mexico at similar elevations yield $\text{T}\Delta_{47}$ values that are within approximately 1°C of MAAT (three carbonate nodules from fine-grained soils sampled by Gallagher and Sheldon, 2016) (Fig. S2). A similar discrepancy can be found by comparing the samples at elevations of about 1000 m on the eastern flank of the Andes: the bias ranges from 0 to 15°C even within samples that are a tens of kilometers apart (samples from Ringham et al. (2016) and Peters et al. (2013)) (Fig. S3), even in a consistent summer precipitation regime. Those authors suggest that landscape position, such as proximity to an active channel and related seasonal flooding, might explain these apparent differences in $\text{T}\Delta_{47}$ (Ringham et al., 2016). These discrepancies between local samples shows the limitation of our understanding of soil carbonate formation.

One explanation for these puzzling differences in apparent seasonal bias could be a mismatch between monitoring data and conditions of carbonate formation (e.g., due to length of record, differing conditions at weather station vs. soil pit, as discussed in Burgener et al. (2018)), but that uncertainty is difficult to quantify.

Another explanation is that the interaction between soil texture, rainfall patterns, vegetation and other factors not yet considered is responsible for the variation of seasonal bias within any single category or geographic location. Unfortunately, limited data availability and poor distribution amongst categories precluded the possibility of a rigorous multivariate statistical analysis in this study (Fig. S4). Regardless, we can make some hypotheses about how these environmental factors would interact to affect seasonal bias. For example, we might predict that the timing of carbonate accumulation is sensitive to the spacing between rain events (Huth et al., 2019) but modulated by soil texture: a certain spacing between rain events might promote soil drying given coarse but not fine-grained soil texture. In other climates, adequately long dry spells might allow for carbonate accumulation during the summer regardless of soil texture, or plentiful summer rain would prevent summertime carbonate formation regardless of soil texture. Snowpack depth and the timing of snowmelt and its percolation into the soil column may be another important factor that is not explicitly considered in this work (Burgener et al., 2016; Peters et al., 2013). The annual timing (and type) of precipitation likely influences vegetative cover and type, which in turn influences soil temperatures and timing of carbonate formation (Meyer et al., 2014).

Future work on understanding $\text{T}\Delta_{47}$ and seasonal bias of soil carbonate formation can be guided by these existing conundrums and data gaps. One outstanding gap in knowledge is a study of soil carbonates from fine grained soils that are better analogs for the soil carbonates found in the geologic record. Furthermore, it would be beneficial to make careful, *in-situ*, measurements of meteorological conditions and soil physical and chemical properties that are collocated with stable isotope data. Experiments that can isolate the environmental factors are also a logical next step to understanding the timing of soil carbonate formation. Such controlled experiments might include numerical modeling of soil physics and

chemistry (Huth et al., 2019), and laboratory and outdoor experiments with controlled environmental conditions. Future work should seek to better understand the process of soil carbonate formation – only then will we be able to unambiguously use the isotopic composition of paleosol carbonates.

5.8. Implications for using pedogenic carbonate for paleoclimate reconstructions

At present, the apparent variations in seasonal biases have prevented the development of a clear framework for how to interpret paleosol carbonate clumped isotope temperatures. Most workers assume a warm-season bias (Burgener et al., 2019; Ghosh et al., 2006b; Hyland et al., 2018; Ingalls et al., 2018; Kelson et al., 2018; Lechler et al., 2018; Snell et al., 2014, 2013; Suarez et al., 2011; Újvári et al., 2019), but detailed considerations of environmental factors that would influence that bias are often not included. Increasingly, researchers recognize a varied seasonal bias in soil carbonate formation either due to environmental factors like monsoon rainfall patterns (Licht et al., 2017), or because a shift in seasonal bias is required to explain observed temperature shifts (Page et al., 2019). As soil carbonate Δ_{47} analysis becomes more common, it is likely that secular changes in seasonal bias of carbonate formation will be encountered – especially considering the large changes in seasonal precipitation patterns that can occur on million-year time scales as a result of changes in atmospheric concentrations of greenhouse gases (Carmichael et al., 2015; Fricke et al., 2010; Sewall and Sloan, 2006) or changes in topography (Huber and Goldner, 2012; Licht et al., 2017, 2014).

This study points to several observations/data that could be used in conjunction with Δ_{47} to bolster interpretations. First, analyzing more than one nodule from a soil horizon will likely increase the fidelity of the temperature estimate, considering that despite variability within a single soil pit, the pit-average usually resembles mean summer air temperature (Burgener et al., 2016; Ringham et al., 2016). Second, major changes in soil texture through a sedimentary record should be taken into consideration when interpreting seasonal bias. Here we show that the limited number of available Holocene soil carbonate samples from fine-grained soils have Δ_{47} values that are similar to MAAT, but Cenozoic soil carbonates from fine-grained paleosols have been interpreted as consistent with MWST (Burgener et al., 2019; Hyland et al., 2018; Kelson et al., 2018). Also, when possible, climate model output could be used to inform relevant precipitation patterns – heavy summer rain will likely result in reduced clumped isotope temperatures (Peters et al., 2013), while sporadic summer rain is likely to result in warm, summer-like clumped isotope temperatures (Huth et al., 2019). Apparent differences in the seasonal bias of modern carbonates collected within tens of kilometers of each other (compare samples collected by Ringham et al. (2016) and Peters et al. (2013)) highlight that robust climate interpretation should rely on analyses of multiple carbonates. The presence of vegetation is likely to reduce Δ_{47} values – either through reducing radiative heating or through changing soil chemistry and hydrology. Radiative heating corrections are unnecessary for carbonates deeper than about 40 cm, especially in densely vegetated landscapes. Lastly, the data in this study show that $\delta^{18}\text{O}_{\text{sw}}$ calculated from $\delta^{18}\text{O}_{\text{c}}$ and Δ_{47} is not necessarily biased toward a seasonal value of rain, even if Δ_{47} values have a strong seasonal bias.

Continued efforts to build a process-based understanding of soil carbonate formation as a function of all the variables explored here will allow future workers to leverage the varied seasonal bias in soil carbonate formation to investigate past temperature seasonality and secular or cyclic change. Paleoclimate reconstructions will be

most robust if specific factors that control bias can be identified in a paleosol, or if soil carbonate Δ_{47} is combined with temperature estimates from other proxies (Burgener et al., 2019; Hyland et al., 2018; Snell et al., 2013).

6. Conclusions

The recalculated dataset compiled here shows that most of the available data from Holocene soil carbonates record Δ_{47} values higher than mean annual air temperature, suggesting that soil carbonates are often representative of mean summer or warm season conditions. However, some Δ_{47} values are within error of mean annual air temperature, and when Δ_{47} exceeds mean annual air temperature that exceedance can be as high as 24 °C. Within the dataset, Δ_{47} does not decrease systematically with depth in the soil, despite the fact that soil temperatures do decrease with depth in the soil during the warm season. Differences in soil texture, seasonal timing of precipitation, and vegetative cover explain some of the variance in apparent seasonal bias in the global dataset. We observed that $\delta^{18}\text{O}_{\text{sw}}$ (calculated from $\delta^{18}\text{O}_{\text{c}}$) appears to be biased toward seasonal rainfall in some environments, but overall is well-correlated with the $\delta^{18}\text{O}$ value of mean annual of precipitation.

For paleoclimate purposes, our analysis suggests that at this point in time Δ_{47} does not represent an easily defined climate parameter such as mean summer temperature or peak summer temperature. Changes in environmental conditions (especially rainfall), substrate grain size, and the presence of vegetation through a sedimentary section should be documented and taken into consideration. Realizing the full potential of clumped isotopes in studies of terrestrial paleoenvironments requires developing a process-based understanding of soil carbonate formation.

Declaration of interests

The authors declare that they have no known competing financial interests or personal relationships that could have appeared to influence the work reported in this paper.

CRediT authorship contribution statement

Julia R. Kelson: Writing - original draft, Conceptualization, Methodology, Investigation, Formal analysis, Funding acquisition. **Katharine W. Huntington:** Conceptualization, Methodology, Writing - review & editing, Funding acquisition. **Daniel O. Breecker:** Conceptualization, Writing - review & editing, Formal analysis, Funding acquisition. **Landon K. Burgener:** Conceptualization, Writing - review & editing, Visualization. **Timothy M. Gallagher:** Conceptualization, Writing - review & editing. **Gregory D. Hoke:** Conceptualization, Writing - review & editing, Funding acquisition, Visualization. **Sierra V. Petersen:** Writing - review & editing, Data curation, Investigation.

Acknowledgements

Thank you to Ben Passey, Majie Fan, Jay Quade and Tyler Huth for providing information about the soil samples they collected and their clumped isotope data. Katie Snell and an anonymous reviewer provided suggestions that improved this paper. JRK completed the work with support from the National Science Foundation Graduate Research Fellowship Program under Grant No. DGE-1256082. Funding also came from National Science Foundation Partnerships for International Research and Education (PIRE) grant 1545859 to DOB, National Science Foundation grants EAR- 1156134 and EAR-1252064 to KWH, and National Science Foundation EAR-1251966 to GDH.

Appendix A. Supplementary data

Supplementary data to this article can be found online at <https://doi.org/10.1016/j.quascirev.2020.106259>.

X-axis is the annual $\delta^{18}\text{O}$ of precipitation (weighted by amount), estimated using the OIPC. X-error bars are 95% confidence interval of the OIPC estimate. Y-error bars are estimated by propagated errors of $\delta^{18}\text{O}_c$ and $\text{T}\Delta_{47}$. The dark gray dashed line is a 1:1 line and the light gray dashed lines are ± 1 , ± 2 , and $\pm 20\%$. Colors indicate seasonal bias of $\delta^{18}\text{O}_{\text{sw}}$ as determined from the normalized residual from $\delta^{18}\text{O}_{\text{ann}}$ (i.e., normalized residual = $(\delta^{18}\text{O}_{\text{sw}} - \delta^{18}\text{O}_{\text{ann}})/(\delta^{18}\text{O}_{\text{max}} - \delta^{18}\text{O}_{\text{ann}})$ where $\delta^{18}\text{O}_{\text{max}}$ is $\delta^{18}\text{O}_{\text{summer}}$ in all cases except for the samples from Tibet where it is $\delta^{18}\text{O}_{\text{winter}}$). A normalized residual value > 0.5 indicates that the $\delta^{18}\text{O}_{\text{sw}}$ is more similar to the $\delta^{18}\text{O}$ of summer rain. A normalized residual value of < 0.5 indicates that the $\delta^{18}\text{O}_{\text{sw}}$ is more similar to the $\delta^{18}\text{O}$ of winter rain. A normalized residual between -0.5 and 0.5 indicates that $\delta^{18}\text{O}_{\text{sw}}$ is most similar to $\delta^{18}\text{O}_{\text{ann}}$. Subplot: kernel density of the normalized residuals from $\delta^{18}\text{O}_{\text{ann}}$.

References

- Allison, G.B., Barnes, C.J., Hughes, M.W., 1983. The distribution of deuterium and ^{18}O in dry soils 2. Exp. J. Hydrol. 64, 377–397. [https://doi.org/10.1016/0022-1694\(83\)90078-1](https://doi.org/10.1016/0022-1694(83)90078-1).
- Amundson, R.G., Chadwick, O.A., Sowers, J.M., Doner, H.E., 1988. Relationship between climate and vegetation and the stable carbon isotope chemistry of soils in the eastern Mojave Desert, Nevada. Quat. Res. 29, 245–254. [https://doi.org/10.1016/0033-5894\(88\)90033-6](https://doi.org/10.1016/0033-5894(88)90033-6).
- Amundson, R.G., Lund, L.J., 1987. The stable isotope chemistry of a native and irrigated typic natrigid in the san joaquin valley of California. Soil Sci. Soc. Am. J. 51, 761–767. <https://doi.org/10.2136/sssaj1987.03615995005100030034x>.
- Arkley, R.J., 1963. Calculation of carbonate and water movement in soil from climatic data. Soil Sci. 96, 239–248. <https://doi.org/10.1097/00010694-196310000-00003>.
- Barnes, C.J., Allison, G.B., 1983. The distribution of deuterium and ^{18}O in dry soils: 1. Theory. J. Hydrol. 60, 141–156. [https://doi.org/10.1016/0022-1694\(83\)90018-5](https://doi.org/10.1016/0022-1694(83)90018-5).
- Bartlett, M.G., Chapman, D.S., Harris, R.N., 2006. A decade of ground-air temperature tracking at emigrant pass observatory, Utah. J. Clim. 19, 3722–3731. <https://doi.org/10.1175/JCLI3808.1>.
- Behrensmeier, A.K., Quade, J., Cerling, T.E., Kappelman, J., Khan, I.A., Copeland, P., Roe, L., Hicks, J., Stubblefield, P., Willis, B.J., Latorre, C., 2007. The structure and rate of late Miocene expansion of C4 plants: evidence from lateral variation in stable isotopes in paleosols of the Siwalik Group, northern Pakistan. Bull. Geol. Soc. Am. 119, 1486–1505. <https://doi.org/10.1130/B26064.1>.
- Birkeland, 1984. Soils and Geomorphology. Oxford University Press.
- Blodgett, R.H., 1988. Calcareous paleosols in the triassic dolores formation, southwestern Colorado. Geol. Soc. Am. Spec. Pap. 216.
- Bonifacie, M., Calmels, D., Eiler, J.M., Horita, J., Chaduteau, C., Vasconcelos, C., Agrinier, P., Katz, A., Passey, B.H., Ferry, J.M., Bourrand, J.-J., 2017. Calibration of the dolomite clumped isotope thermometer from 25 to 350 °C, and implications for a universal calibration for all (Ca, Mg, Fe)CO₃ carbonates. Geochim. Cosmochim. Acta 200, 255–279. <https://doi.org/10.1016/j.gca.2016.11.028>.
- Borken, W., Davidson, E.A., Savage, K., Gaudinski, J., Trumbore, S.E., 2003. Drying and wetting effects on carbon dioxide release from organic horizons. Soil Sci. Soc. Am. J. 67, 1888–1896. <https://doi.org/10.2136/sssaj2003.1888>.
- Bouma, T.J., Bryla, D.R., 2000. On the assessment of root and soil respiration for soils of different textures: interactions with soil moisture contents and soil CO₂ concentrations. Plant Soil 227, 215–221. <https://doi.org/10.1023/A:1026502414977>.
- Bowen, G.J., Revenaugh, J., 2003. Interpolating the isotopic composition of modern meteoric precipitation. Water Resour. Res. 39. <https://doi.org/10.1029/2003WR002086>.
- Bowling, D.R., Grote, E.E., Belnap, J., 2011. Rain pulse response of soil CO₂ exchange by biological soil crusts and grasslands of the semiarid Colorado Plateau, United States. J. Geophys. Res. Biogeosci. 116, 1–17. <https://doi.org/10.1029/2011JG001643>.
- Brand, W., Assonov, S.S., Coplen, T.B., 2010. Correction for the 17O interference in $\delta^{13}\text{C}$ measurements when analyzing CO₂ with stable isotope mass spectrometry (IUPAC Technical Report). Pure Appl. Chem. 82, 1719–1733. <https://doi.org/10.1351/PAC-REP-09-01-05>.
- Breecker, D.O., McFadden, L.D., Sharp, Z.D., Martinez, M., Litvak, M.E., 2012. Deep autotrophic soil respiration in shrubland and woodland ecosystems in central New Mexico. Ecosystems 15, 83–96. <https://doi.org/10.1007/s10021-011-9495-x>.
- Breecker, D.O., Sharp, Z.D., McFadden, L.D., 2009. Seasonal bias in the formation and stable isotopic composition of pedogenic carbonate in modern soils from central New Mexico, USA. Bull. Geol. Soc. Am. 121, 630–640. <https://doi.org/10.1130/B26413.1>.
- Breshears, D.D., Nyhan, J.W., Heil, C.E., Wilcox, B.P., 1998. Effects of woody plants on microclimate in a semiarid woodland: soil temperature and evaporation in canopy and intercanopy patches. Int. J. Plant Sci. 159, 1010–1017. <https://doi.org/10.1086/314083>.
- Burgener, L.K., Huntington, K.W., Hoke, G.D., Schauer, A.J., Ringham, M.C., Latorre, C., Diaz, F.P., 2016. Variations in soil carbonate formation and seasonal bias over >4 km of relief in the western Andes (30°S) revealed by clumped isotope thermometry. Earth Planet. Sci. Lett. 441, 188–199. <https://doi.org/10.1016/j.epsl.2016.02.033>.
- Burgener, L.K., Huntington, K.W., Sletten, R., Watkins, J.M., Quade, J., Hallet, B., 2018. Clumped isotope constraints on equilibrium carbonate formation and kinetic isotope effects in freezing soils. Geochim. Cosmochim. Acta 235, 402–430. <https://doi.org/10.1016/j.gca.2018.06.006>.
- Burgener, L.K., Hyland, E.G., Huntington, K.W., Kelson, J.R., Sewall, J.O., 2019. Revisiting the equable climate problem during the Late Cretaceous greenhouse using paleosol carbonate clumped isotope temperatures from the Campanian of the Western Interior Basin, USA. Palaeogeogr. Palaeoclimatol. Palaeoecol. 516, 244–267. <https://doi.org/10.1016/j.palaeo.2018.12.004>.
- Carmichael, M.J., Lunt, D.J., Pancost, R.D., 2015. Insights into the early Eocene hydrological cycle from an ensemble of atmosphere-ocean GCM simulations. Clim. Past Discuss 17, 8839. <https://doi.org/10.5194/cpd-11-3277-2015>.
- Carsel, R.F., Parrish, R.S., 1988. Developing joint probability distributions of soil water retention characteristics. Water Resour. Res. Res. 24, 755–769.
- Caves, J.K., Moragne, D.Y., Ibarra, D.E., Bayshashov, B.U., Gao, Y., Jones, M.M., Zhamangara, A., Arzhannikova, A.V., Arzhannikov, S.G., Chamberlain, C.P., 2016. The neogene de-greening of central Asia. Geology 44, 887–890. <https://doi.org/10.1130/G38267.1>.
- Caves Rugenstein, J.K., Chamberlain, C.P., 2018. The evolution of hydroclimate in Asia over the Cenozoic: a stable-isotope perspective. Earth Sci. Rev. 185, 1129–1156. <https://doi.org/10.1016/j.earscirev.2018.09.003>.
- Cerling, T.E., 1984. The stable isotopic composition of modern soil carbonate and its relation to climate. Earth Planet. Sci. Lett. 71, 229–240.
- Cerling, T.E., Hay, R.L., 1986. An isotopic study of paleosol carbonates from Olduvai Gorge. Quat. Res. 25, 63–78.
- Cerling, T.E., Quade, J., 1993. Stable carbon and oxygen isotopes in soil carbonates. Geophys. Monogr. 78, 217–231. <https://doi.org/10.1029/GM078p0217>.
- Cerling, T.E., Quade, J., Wang, Y., Bowman, J.R., 1989. Carbon isotopes in soils and paleosols as ecology and palaeoecology indicators. Nature 341, 138–139. <https://doi.org/10.1038/341138a0>.
- Cerling, T.E., Solomon, D.K., Quade, J., Bowman, J.R., 1991. On the isotopic composition of carbon in soil carbon dioxide. Geochim. Cosmochim. Acta 55, 3403–3405. [https://doi.org/10.1016/0016-7037\(91\)90498-T](https://doi.org/10.1016/0016-7037(91)90498-T).
- Cermak, V., Bodri, L., Kresl, M., Dedecek, P., Safanda, J., 2017. Eleven years of ground-air temperature tracking over different land cover types. Int. J. Climatol. 37, 1084–1099. <https://doi.org/10.1002/joc.4764>.
- Coplen, T.B., 2007. Calibration of the calcite-water oxygen-isotope geothermometer at Devils Hole, Nevada, a natural laboratory. Geochim. Cosmochim. Acta 71, 3948–3957. <https://doi.org/10.1016/j.gca.2007.05.028>.
- Da, J., Zhang, Y.G., Li, G., Meng, X., Ji, J., 2019. Low CO₂ levels of the entire Pleistocene epoch. Nat. Commun. 10, 1–9. <https://doi.org/10.1038/s41467-019-12357-5>.
- Daéron, M., Blamart, D., Peral, M., Affek, H.P., 2016. Absolute isotopic abundance ratios and the accuracy of Δ_{47} measurements. Chem. Geol. 442, 83–96. <https://doi.org/10.1016/j.chemgeo.2016.08.014>.
- Dennis, K.J., Affek, H.P., Passey, B.H., Schrag, D.P., Eiler, J.M., 2011. Defining an absolute reference frame for ‘clumped’ isotope studies of CO₂. Geochim. Cosmochim. Acta 75, 7117–7131. <https://doi.org/10.1016/j.gca.2011.09.025>.
- Ding, Z.L., Yang, S.L., 2000. C3/C4 vegetation evolution over the last 7.0 Myr in the Chinese Loess Plateau: evidence from pedogenic carbonate $\delta^{13}\text{C}$. Palaeogeogr. Palaeoclimatol. Palaeoecol. 160, 291–299. [https://doi.org/10.1016/S0031-0182\(00\)00076-6](https://doi.org/10.1016/S0031-0182(00)00076-6).
- Drever, J.L., 1982. The Geochemistry of Natural Waters. Prentice Hall, New York.
- Durand, N., Monger, H.C., Canti, M.G., Verrecchia, E.P., 2010. Calcium carbonate features. In: Stoops, G., Marcelino, V., Mees, F. (Eds.), Interpretation of Micro-morphological Features of Soils and Regoliths. Elsevier, pp. 149–194.
- Dworkin, S.L., Nordt, L.C., Atchley, S.C., 2005. Determining terrestrial paleotemperatures using the oxygen isotopic composition of pedogenic carbonate. Earth Planet. Sci. Lett. 237, 56–68. <https://doi.org/10.1016/j.epsl.2005.06.054>.
- Eagle, R.A., Risi, C., Mitchell, J.L., Eiler, J.M., Seibt, U., Neelin, J.D., Li, G., Tripathi, A.K., 2013. High regional climate sensitivity over continental China constrained by glacial-recent changes in temperature and the hydrological cycle. Proc. Natl. Acad. Sci. U.S.A. 110, 8813–8818. <https://doi.org/10.1073/pnas.1213366110>.
- Eiler, J.M., 2011. Paleoclimate reconstruction using carbonate clumped isotope thermometry. Quat. Sci. Rev. 30, 3575–3588. <https://doi.org/10.1016/j.quascirev.2011.09.001>.
- Eiler, J.M., 2007. “Clumped-isotope” geochemistry—the study of naturally-occurring, multiply-substituted isotopologues. Earth Planet. Sci. Lett. 262, 309–327. <https://doi.org/10.1016/j.epsl.2007.08.020>.
- Ekart, D.D., Cerling, T.E., Montañez, I.P., Tabor, N.J., 1999. A 400 million year carbon isotope record of pedogenic carbonate: implications for paleoatmospheric carbon dioxide. Am. J. Sci. <https://doi.org/10.2475/ajs.299.10.805>.
- Fan, M., Carrapa, B., 2014. Late Cretaceous – early Eocene Laramide uplift, exhumation, and basin subsidence in Wyoming: crustal responses to fl at slab subduction. Tectonics 509–529. <https://doi.org/10.1002/2012TC003221>.Received.

- Fernandez, A., Müller, I.A., Rodríguez-Sanz, L., van Dijk, J., Looser, N., Bernasconi, S.M., 2017. A reassessment of the precision of carbonate clumped isotope measurements: implications for calibrations and paleoclimate reconstructions. *Geochemistry, Geophys. Geosystems* 1–12. <https://doi.org/10.1002/2017GC007106>.
- Fox, D.L., Koch, P.L., 2004. Carbon and oxygen isotopic variability in Neogene paleosol carbonates: constraints on the evolution of the C4-grasslands of the Great Plains, USA. *Palaeogeogr. Palaeoclimatol. Palaeoecol.* 207, 305–329. <https://doi.org/10.1016/j.palaeo.2003.09.030>.
- Fredlund, D.G., Xing, A., 1994. Equations for the soil-water characteristic curve. *Can. Geotech. J.* 31, 521–532.
- Fricke, H.C., Foreman, B.Z., Sewall, J.O., 2010. Integrated climate model-oxygen isotope evidence for a North American monsoon during the Late Cretaceous. *Earth Planet. Sci. Lett.* 289, 11–21. <https://doi.org/10.1016/j.epsl.2009.10.018>.
- Friedl, M.A., Sulla-Menashe, D., Tan, B., Schneider, A., Ramankutty, N., Sibley, A., Huang, X., 2010. MODIS Collection 5 global land cover: algorithm refinements and characterization of new datasets. *Remote Sens. Environ.* 114, 168–182. <https://doi.org/10.1016/j.rse.2009.08.016>.
- Gallagher, T.M., Hren, M.T., Sheldon, N.D., 2019. The effect of soil temperature seasonality on climate reconstructions from paleosols. *Am. J. Sci.* 319, 549–581. <https://doi.org/10.2475/07.2019.02>.
- Gallagher, T.M., Sheldon, N.D., 2016. Combining soil water balance and clumped isotopes to understand the nature and timing of pedogenic carbonate formation. *Chem. Geol.* 435, 79–91. <https://doi.org/10.1016/j.chemgeo.2016.04.023>.
- Garziane, C.N., Auerbach, D.J., Jin-Sook Smith, J., Rosario, J.J., Passey, B.H., Jordan, T.E., Eiler, J.M., 2014. Clumped isotope evidence for diachronous surface cooling of the Altiplano and pulsed surface uplift of the Central Andes. *Earth Planet. Sci. Lett.* 393, 173–181. <https://doi.org/10.1016/j.epsl.2014.02.029>.
- Garziane, C.N., Quade, J., DeCelles, P.G., English, N.B., 2000. Predicting paleoelevation of Tibet and the Himalaya from $\delta^{18}\text{O}$ vs. altitude gradients in meteoric water across the Nepal Himalaya. *Earth Planet. Sci. Lett.* 183, 215–229. [https://doi.org/10.1016/S0012-821X\(00\)00252-1](https://doi.org/10.1016/S0012-821X(00)00252-1).
- Gaziz, C., Feng, X., 2004. A stable isotope study of soil water: evidence for mixing and preferential flow paths. *Geoderma* 119, 97–111. [https://doi.org/10.1016/S0016-7061\(03\)00243-X](https://doi.org/10.1016/S0016-7061(03)00243-X).
- Gehrels, J.C., Peeters, J.E.M., De Vries, J.J., Dekkers, M., 1998. The mechanism of soil water movement as inferred from ^{18}O stable isotope studies. *Hydrol. Sci. J.* 43, 579–594. <https://doi.org/10.1080/02626669809492154>.
- Geiger, R., Aron, R.H., Todhunter, P., 2009. *The Climate Near the Ground*, seventh ed. Rowman & Littlefield.
- Ghosh, P., Adkins, J.F., Affek, H.P., Balta, B., Guo, W., Schauble, E.A., Schrag, D.P., Eiler, J.M., 2006a. ^{13}C – ^{18}O bonds in carbonate minerals: a new kind of paleothermometer. *Geochem. Cosmochim. Acta* 70, 1439–1456. <https://doi.org/10.1016/j.gca.2005.11.014>.
- Ghosh, P., Garziane, C.N., Eiler, J.M., 2006b. Rapid uplift of the altiplano revealed through ^{13}C – ^{18}O bonds in paleosol carbonates. *Science* 311, 511–515. <https://doi.org/10.1126/science.1119365>.
- Gile, L.H., Peterson, F.F., Grossman, R.B., 1966. Morphological and genetic sequences of carbonate accumulation in desert soils. *Soil Sci.* 101, 347–360.
- Gocke, M., Pustovoytov, K., Muzyakov, Y., 2012. Pedogenic carbonate formation: recrystallization versus migration process rates and periods assessed by ^{14}C labeling. *Global Biogeochem. Cycles* 26, 1–12. <https://doi.org/10.1029/2010GB003871>.
- Harden, J.W., Taylor, E.M., Hill, C., Mark, R.K., McFadden, L.D., Reheis, M.C., Sowers, J.M., Wells, S.G., 1991. Rates of soil development from four soil chronosequences in the southern Great Basin. *Quat. Res.* 35, 383–399. [https://doi.org/10.1016/0033-5894\(91\)90052-7](https://doi.org/10.1016/0033-5894(91)90052-7).
- Hillel, D., 1982. *Introduction to Soil Physics*. Academic Press, Inc.
- Hoke, G.D., Aranibar, J.N., Viale, M., Araneo, D.C., Llano, C., 2013. Seasonal moisture sources and the isotopic composition of precipitation, rivers, and carbonates across the Andes at 32.5 – 35.5°S . *Geochemistry, Geophys. Geosystems* 14, 962–978. <https://doi.org/10.1002/ggge.20045>.
- Hoke, G.D., Garziane, C.N., Araneo, D.C., Latorre, C., Strecker, M.R., Williams, K.J., 2009. The stable isotope altimeter: do Quaternary pedogenic carbonates predict modern elevations? *Geology* 37, 1015–1018. <https://doi.org/10.1130/G30308A.1>.
- Hough, B.G., Fan, M., Passey, B.H., 2014. Calibration of the clumped isotope geothermometer in soil carbonate in Wyoming and Nebraska, USA: implications for paleoelevation and paleoclimate reconstruction. *Earth Planet. Sci. Lett.* 391. <https://doi.org/10.1016/j.epsl.2014.01.008>.
- Hsieh, J.C.C., Chadwick, O.A., Kelly, E.F., Savin, S.M., 1998. Oxygen isotopic composition of soil water: quantifying evaporation and transpiration. *Geoderma* 82, 269–293. [https://doi.org/10.1016/S0016-7061\(97\)00105-5](https://doi.org/10.1016/S0016-7061(97)00105-5).
- Huber, M., Goldner, A., 2012. Eocene monsoons. *J. Asian Earth Sci.* 44, 3–23. <https://doi.org/10.1016/j.jseas.2011.09.014>.
- Huntington, K.W., Eiler, J.M., Affek, H.P., Guo, W., Bonifacie, M., Yeung, L.Y., Thiagarajan, N., Passey, B.H., Tripathi, A.K., Daéron, M., Came, R.E., 2009. Methods and limitations of “clumped” CO_2 isotope ($\Delta 47$) analysis by gas-source isotope ratio mass spectrometry. *J. Mass Spectrom.* 44, 1318–1329. <https://doi.org/10.1002/jms.1614>.
- Huntington, K.W., Lechler, A.R., 2015. Carbonate clumped isotope thermometry in continental tectonics. *Tectonophysics* 647–648, 1–20. <https://doi.org/10.1016/j.tecto.2015.02.019>.
- Huth, T.E., Cerling, T.E., Marchetti, D.W., Bowling, D.R., Ellwein, A.L., Passey, B.H., 2019. Seasonal bias in soil carbonate formation and its implications for interpreting high-resolution paleoarchives: evidence from southern Utah. *J. Geophys. Res. Biogeosci.* 124, 616–632. <https://doi.org/10.1029/2018JG004496>.
- Hyland, E.G., Huntington, K.W., Sheldon, N.D., Reichgelt, T., 2018. Temperature seasonality in the North American continental interior during the early Eocene climatic optimum, 2018. *Clim. Past Discuss.* 1–39. <https://doi.org/10.5194/cp-2018-28>.
- Ingalls, M., Rowley, D.B., Olack, G.A., Currie, B., Li, S., Schmidt, J., Tremblay, M., Polissar, P., Shuster, D.L., Lin, D., Colman, A.S., 2018. Paleocene to Pliocene low-latitude, high-elevation basins of southern Tibet: implications for tectonic models of India-Asia collision, Cenozoic climate, and geochemical weathering. *Bull. Geol. Soc. Am.* 130, 307–330. <https://doi.org/10.1130/B31723.1>.
- Inskeep, W.P., Bloom, P.R., 1986. Kinetics of calcite precipitation in the presence of water-soluble organic ligands. *Soil Sci. Soc. Am. J.* 50, 1167–1172.
- Jenny, H., 1941. *Factors of Soil Formation: A System of Quantitative Pedology*. McGraw-Hill Book Company, New York.
- Ji, S., Nie, J., Lechler, A.R., Huntington, K.W., Heitmann, E.O., Breecker, D.O., 2018. A symmetrical CO_2 peak and asymmetrical climate change during the middle Miocene. *Earth Planet. Sci. Lett.* 499, 134–144. <https://doi.org/10.1016/j.epsl.2018.07.011>.
- Kaakinen, A., Sonninen, E., Lunkka, J.P., 2006. Stable isotope record in paleosol carbonates from the Chinese Loess Plateau: implications for late Neogene paleoclimate and paleovegetation. *Palaeogeogr. Palaeoclimatol. Palaeoecol.* 237, 359–369. <https://doi.org/10.1016/j.palaeo.2005.12.011>.
- Kaufmann, R.K., Zhou, L., Myneni, R.B., Tucker, C.J., Slayback, D., Shabanov, N.V., Pinzon, J., 2003. The effect of vegetation on surface temperature: a statistical analysis of NDVI and climate data. *Geophys. Res. Lett.* 30, 3–6. <https://doi.org/10.1029/2003GL018251>.
- Kele, S., Breitenbach, S.F.M., Capezuoli, E., Meckler, A.N., Ziegler, M., Millan, I.M., Kluge, T., Deák, J., Hanselmann, K., John, C.M., Yan, H., Liu, Z., Bernasconi, S.M., 2015. Temperature dependence of oxygen- and clumped isotope fractionation in carbonates: a study of travertines and tufas in the 6 – 95°C temperature range. *Geochem. Cosmochim. Acta* 168, 172–192. <https://doi.org/10.1016/j.gca.2015.06.032>.
- Kelson, J.R., Huntington, K.W., Schauer, A.J., Saenger, C., Lechler, A.R., 2017. Toward a universal carbonate clumped isotope calibration: diverse synthesis and preparatory methods suggest a single temperature relationship. *Geochem. Cosmochim. Acta* 197. <https://doi.org/10.1016/j.gca.2016.10.010>.
- Kelson, J.R., Watford, D., Bataille, C.P., Huntington, K.W., Hyland, E.G., Bowen, G.J., 2018. Warm terrestrial subtropics during the paleocene and eocene: carbonate clumped isotope ($\Delta 47$) evidence from the tornillo basin, Texas (USA). *Paleoceanogr. Paleoclimatology* 1–20. <https://doi.org/10.1029/2018PA003391>.
- Kim, S.T., O’Neil, J.R., 1997. Equilibrium and nonequilibrium oxygen isotope effects in synthetic carbonates. *Geochem. Cosmochim. Acta* 61, 3461–3475. [https://doi.org/10.1016/S0016-7037\(97\)00169-5](https://doi.org/10.1016/S0016-7037(97)00169-5).
- Koch, P.L., Zachos, J.C., Dettman, D.L., 1995. Stable isotope stratigraphy and paleoclimatology of the paleogene bighorn basin (Wyoming, USA). *Palaeogeogr. Palaeoclimatol. Palaeoecol.* 115, 61–89. [https://doi.org/10.1016/0031-0182\(94\)00107-J](https://doi.org/10.1016/0031-0182(94)00107-J).
- Lebrón, I., Suárez, D.L., 1998. Kinetics and mechanisms of precipitation of calcite as affected by PCO_2 and organic ligands at 25°C . *Geochem. Cosmochim. Acta* 62, 405–416. [https://doi.org/10.1016/S0016-7037\(97\)00364-5](https://doi.org/10.1016/S0016-7037(97)00364-5).
- Lechler, A.R., Huntington, K.W., Breecker, D.O., Sweeney, M.R., Schauer, A.J., 2018. Loess–paleosol carbonate clumped isotope record of late Pleistocene–Holocene climate change in the Palouse region, Washington State, USA. *Quat. Res.* 1–17. <https://doi.org/10.1017/qua.2018.47>.
- Lechler, A.R., Niemi, N.A., Hren, M.T., Lohmann, K.C., 2013. Paleoelevation estimates for the northern and central proto-Basin and Range from carbonate clumped isotope thermometry. *Tectonics* 32. <https://doi.org/10.1002/tect.20016>.
- Lee, X., Wu, H.-J., Sigler, J., Oishi, C., Siccarda, T., 2004. Rapid and transient response of soil respiration to rain. *Global Change Biol.* 10, 1017–1026. <https://doi.org/10.1111/j.1365-2486.2004.00787.x>.
- Leier, A., McQuarrie, N., Garziane, C.N., Eiler, J.M., 2013. Stable isotope evidence for multiple pulses of rapid surface uplift in the Central Andes, Bolivia. *Earth Planet. Sci. Lett.* 371–372, 49–58. <https://doi.org/10.1016/j.epsl.2013.04.025>.
- Levin, N.E., Brown, F.H., Behrensmeier, A.K., Bobe, R., Cerling, T.E., 2011. Paleosol carbonates from the omo group: isotopic records of local and regional environmental change in east africa. *Palaeogeogr. Palaeoclimatol. Palaeoecol.* 307, 75–89. <https://doi.org/10.1016/j.palaeo.2011.04.026>.
- Levin, N.E., Zipser, E.J., Ceding, T.E., 2009. Isotopic composition of waters from Ethiopia and Kenya: insights into moisture sources for eastern Africa. *J. Geophys. Res. Atmos.* 114, 1–13. <https://doi.org/10.1029/2009JD012166>.
- Levitt, N.P., Eiler, J.M., Romanek, C.S., Beard, B.L., Xu, H., Johnson, C.M., 2018. Near equilibrium ^{13}C – ^{18}O bonding during inorganic calcite precipitation under chemo-stat conditions. *Geochemistry, Geophys. Geosystems*. <https://doi.org/10.1002/2017GC007089>.
- Li, Y., Zhang, W., Aydin, A., Deng, X., 2018. Formation of calcareous nodules in loess–paleosol sequences: reviews of existing models with a proposed new “per evapotranspiration model”. *J. Asian Earth Sci.* 154, 8–16. <https://doi.org/10.1016/j.jseas.2017.12.002>.
- Licht, A., Quade, J., Kowler, A., De Los Santos, M., Hudson, A.M., Schauer, A.J., Huntington, K.W., Copeland, P., Lawton, T.F., 2017. Impact of the North American monsoon on isotope paleoaltimeters: implications for the paleoaltimetry of the American southwest. *Am. J. Sci.* 317, 1–33. <https://doi.org/10.2475/10.2475.01.2017.01>.
- Licht, A., Van Cappelle, M., Abels, H.A., Ladant, J.-B., Trabucho-Alexandre, J., France-Lanord, C., Donnadieu, Y., Vandenbergh, J., Rigaudier, T., Lécuyer, C., Terry, D.,

- Adriaens, R., Boura, A., Guo, Z., Soe, A.N., Quade, J., Dupont-Nivet, G., Jaeger, J.J., 2014. Asian monsoons in a late Eocene greenhouse world. *Nature* 513, 501–506. <https://doi.org/10.1038/nature13704>.
- Liu, B., Phillips, F.M., Campbell, A.R., 1996. Stable carbon and oxygen isotopes of pedogenic carbonates, Ajo Mountains, southern Arizona: implications for paleoenvironmental change. *Palaeogeogr. Palaeoclimatol. Palaeoecol.* 124, 233–246. [https://doi.org/10.1016/0031-0182\(95\)00093-3](https://doi.org/10.1016/0031-0182(95)00093-3).
- Liu, X., Wan, S., Su, B., Hui, D., Luo, Y., 2002. Response of soil CO₂ efflux to water manipulation in a tallgrass prairie ecosystem. *Plant Soil* 240, 213–223. <https://doi.org/10.1023/A:1015744126533>.
- Machette, M.N., 1985. Calcic soils of the southwestern United States. In: Weide, D.L. (Ed.), *Soils and Quaternary Geology of the Southwestern United States*. Geological Society of America. <https://doi.org/10.1130/SPE203>.
- Marion, G.M., Schlesinger, W.H., 1994. Quantitative modeling of soil forming processes in deserts: the CALDEP and CALGYP models. *Quant. Model. Soil Form. Process.* 129–145.
- Marion, G.M., Verburg, P.S.J., Stevenson, B., Arnone, J.A., 2008. Soluble element distributions in a Mojave desert soil. *Soil Sci. Soc. Am. J.* 72, 1815–1824. <https://doi.org/10.2136/sssaj2007.0240>.
- Mathieu, R., Bariac, T., 1996. An isotopic study (2H and 18O) of water movements in clayey soils under a semiarid climate. *Waster Resour. Res.* 32, 779–789.
- McDonald, E.V., Pierson, F.B., Flerchinger, G.N., McFadden, L.D., 1996. Application of a soil-water balance model to evaluate the influence of holocene climate change on calcic soils, Mojave Desert, California. *U.S.A. Geoderma* 74, 167–192. [https://doi.org/10.1016/S0016-7061\(96\)00070-5](https://doi.org/10.1016/S0016-7061(96)00070-5).
- McFadden, L.D., 2013. Strongly dust-influenced soils and what they tell us about landscape dynamics in vegetated aridlands of the southwestern United States. *Geol. Soc. Am. Spec. Pap.* 500, 501–532. <https://doi.org/10.1130/2013.250015>.
- McFadden, L.D., Amundson, R.G., Chadwick, O.A., 1991. Numerical modeling chemical, and isotopic studies of carbonate accumulation in arid regions. *Occur. Charact. Genes. Carbonate, Gypsum, Silica Accumulations soils* 17–35.
- McFadden, L.D., Tinsley, J.C., 1985. Rate and depth of pedogenic-carbonate accumulation in soils: formulation and testing of a compartment model. *Geol. Soc. Am. Spec. Pap.* 203.
- Methner, K., Mulch, A., Fiebig, J., Wacker, U., Gerdes, A., Graham, S.A., Chamberlain, C.P., 2016. Rapid middle eocene temperature change in western North America. *Earth Planet Sci. Lett.* 450, 132–139. <https://doi.org/10.1016/j.epsl.2016.05.053>.
- Meyer, N.A., Breecker, D.O., Young, M.H., Litvak, M.E., 2014. Simulating the effect of vegetation in formation of pedogenic carbonate. *Soil Sci. Soc. Am. J.* 78, 914. <https://doi.org/10.2136/sssaj2013.08.0326>.
- Monger, H.C., Cole, D.R., Buck, B.J., Gallegos, R.A., 2009. Scale and the isotopic record of C4 plants in pedogenic carbonate: from the biome to the rhizosphere. *Ecology* 90, 1498–1511. <https://doi.org/10.1890/08-0670.1>.
- Monger, H.C., Cole, D.R., Gish, J., Giordano, T., 1998. Stable carbon and oxygen isotopes in Quaternary soil carbonates as indicators of ecogeomorphic changes in the northern Chihuahuan Desert, USA. *Geoderma* 82, 137–172. [https://doi.org/10.1016/S0016-7061\(97\)00100-6](https://doi.org/10.1016/S0016-7061(97)00100-6).
- Monger, H.C., Daugherty, L.A., Lindemann, W.C., 1991. Microbial precipitation of pedogenic calcite. *Geology* 19, 997–1000. [https://doi.org/10.1130/0091-7613\(1991\)019<0997:MPOPC>2.3.CO](https://doi.org/10.1130/0091-7613(1991)019<0997:MPOPC>2.3.CO). [https://doi.org/10.1130/0091-7613\(1991\)019%3c0997:MPOPC%3e2.3.CO;2](https://doi.org/10.1130/0091-7613(1991)019%3c0997:MPOPC%3e2.3.CO;2).
- Müller, I.A., Fernandez, A., Radke, J., van Dijk, J., Bowen, D., Schwieters, J., Bernasconi, S.M., 2017. Carbonate clumped isotope analyses with the long-integration dual-inlet (LIDI) workflow: scratching at the lower sample weight boundaries. *Rapid Commun. Mass Spectrom.* 31. <https://doi.org/10.1002/rcm.7878>.
- Nordt, L.C., Atchley, S.C., Dworkin, S.I., 2003. Terrestrial Evidence for Two Greenhouse Events in the Latest Cretaceous, vol. 13. *GSA Today*, pp. 4–9. [https://doi.org/10.1130/1052-5173\(2003\)013<4:TEFTGE>2.0.CO;2](https://doi.org/10.1130/1052-5173(2003)013<4:TEFTGE>2.0.CO;2).
- Noy-Meir, I., 1973. Desert ecosystems: environment and producers. *Annu. Rev. Ecol. Systemat.* 25–51.
- Oerter, E.J., Amundson, R.G., 2016. Climate controls on spatial temporal variations in the formation of pedogenic carbonate in the western Great Basin of North America. *Bull. Geol. Soc. Am.* 128, 1095–1104. <https://doi.org/10.1130/B31367.1>.
- Oshun, J., Dietrich, W.E., Dawson, T.E., Fung, I., 2015. Dynamic, structured heterogeneity of water isotopes inside hillslopes. *Water Resour. Res.* 2616–2633. <https://doi.org/10.1002/2015WR017485>.
- Page, M., Licht, A., Dupont-Nivet, G., Meijer, N., Barbolini, N., Hoorn, C., Schauer, A.J., Huntington, K.W., Bajnai, D., Fiebig, J., Mulch, A., Guo, Z., 2019. Synchronous cooling and decline in monsoonal rainfall in northeastern Tibet during the fall into the Oligocene icehouse. *Geology* 47, 203–206. <https://doi.org/10.1130/g45480.1>.
- Passey, B.H., 2012. Reconstructing terrestrial environments using stable isotopes in fossil teeth and paleosol carbonates. *Paleontol. Soc. Pap.* 18.
- Passey, B.H., Levin, N.E., Cerling, T.E., Brown, F.H., Eiler, J.M., 2010. High-temperature environments of human evolution in East Africa based on bond ordering in paleosol carbonates. *Proc. Natl. Acad. Sci. U.S.A.* 107, 11245–11249. <https://doi.org/10.1073/pnas.1001824107>.
- Peral, M., Daëron, M., Blamart, D., Bassinot, F., Dewilde, F., Smialkowski, N., Isguder, G., Bonnin, J., Jorissen, F., Kissel, C., Michel, E., Vázquez Riveiros, N., Waelbroeck, C., 2018. Updated calibration of the clumped isotope thermometer in planktonic and benthic foraminifera. *Geochim. Cosmochim. Acta* 239, 1–16. <https://doi.org/10.1016/j.gca.2018.07.016>.
- Peters, N.A., Huntington, K.W., Hoke, G.D., 2013. Hot or not? Impact of seasonally variable soil carbonate formation on paleotemperature and O-isotope records from clumped isotope thermometry. *Earth Planet Sci. Lett.* 361, 208–218. <https://doi.org/10.1016/j.epsl.2012.10.024>.
- Petersen, S.V., Defliese, W.F., Saenger, C., Daëron, M., Huntington, K.W., John, C.M., Kelson, J.R., Bernasconi, S.M., Colman, A.S., Kluge, T., Olack, G.A., Schauer, A.J., Bajnai, D., Bonifacie, M., Breitenbach, S.F.M., Fiebig, J., Fernandez, A.B., Henkes, G.A., Hodell, D., Katz, A., Kele, S., Lohmann, K.C., Passey, B.H., Peral, M.Y., Petrizzo, D.A., Rosenheim, B.E., Tripati, A., Venturilli, R., Young, E.D., Winkelstern, I.Z., 2019. Effects of improved 17 O correction on interlaboratory agreement in clumped isotope calibrations, estimates of mineral-specific offsets, and temperature dependence of acid digestion fractionation. *Geochemistry, Geophysics. Geosystems* 3495–3519. <https://doi.org/10.1029/2018gc008127>.
- Quade, J., Breecker, D.O., Daëron, M., Eiler, J.M., 2011. The paleothermometry of Tibet: an isotopic perspective. *Am. J. Sci.* 311, 77–115. <https://doi.org/10.2475/02.2011.01>.
- Quade, J., Cater, J.M.L., Ojha, T.P., Adam, J., Harrison, T.M., Erdei, B., Hir, J., 1995. Late Miocene Environmental Change in Nepal and the Northern Indian Subcontinent: Stable Isotopic Evidence from Paleosols. *Vegetation and Climate Reconstruction of Sarmatian (Middle Miocene) Sites from NE and W Hungary*, vol. 107, pp. 1381–1397.
- Quade, J., Cerling, T.E., Bowman, J.R., 1989. Systematic variations in the carbon and oxygen isotopic composition of pedogenic carbonate along elevation transects in the southern Great Basin, United States. *Geol. Soc. Am. Bull.* 101, 464–475. [https://doi.org/10.1130/0016-7606\(1989\)101%3c0464:SVITCA%3e2.3.CO;2](https://doi.org/10.1130/0016-7606(1989)101%3c0464:SVITCA%3e2.3.CO;2).
- Quade, J., Eiler, J.M., Daëron, M., Achyuthan, H., 2013. The clumped isotope geothermometer in soil and paleosol carbonate. *Geochim. Cosmochim. Acta* 105, 92–107. <https://doi.org/10.1016/j.gca.2012.11.031>.
- Quade, J., Garzione, C.N., Eiler, J.M., 2007. Paleoelevation reconstruction using pedogenic carbonates. *Rev. Mineral. Geochem.* 66, 53–87. <https://doi.org/10.2138/rmg.2007.66.3>.
- Radcliffe, D.E., Šimůnek, J., 2010. *Soil Physics with HYDRUS: Modeling and Applications*. CRC press.
- Retallack, G.J., 2005. Pedogenic carbonate proxies for amount and seasonality of precipitation in paleosols. *Geology* 33, 333–336. <https://doi.org/10.1130/G21263.1>.
- Ringham, M.C., Hoke, G.D., Huntington, K.W., Aranibar, J.N., 2016. Influence of vegetation type and site-to-site variability on soil carbonate clumped isotope records, Andean piedmont of Central Argentina (32–34°S). *Earth Planet Sci. Lett.* 440, 1–11. <https://doi.org/10.1016/j.epsl.2016.02.003>.
- Salomons, W., Mook, W.G., 1986. Isotope geochemistry of carbonates in the weathering zone. In: Fritz, P., Fontes, J.C. (Eds.), *Handbook of Environmental Isotope Geochemistry, The Terrestrial Environment*, vol. 2. Elsevier B.V., Amsterdam, pp. 239–269. <https://doi.org/10.1016/b978-0-444-42225-5.50011-5>.
- Santrock, J., Studley, S.A., Hayes, J.M., 1985. Isotopic analyses based on the mass spectrum of carbon dioxide. *Anal. Chem.* 57, 1444–1448. <https://doi.org/10.1021/ac00284a060>.
- Schauble, E.A., Ghosh, P., Eiler, J.M., 2006. Preferential formation of 13C–18O bonds in carbonate minerals, estimated using first-principles lattice dynamics. *Geochim. Cosmochim. Acta* 70, 2510–2529. <https://doi.org/10.1016/j.gca.2006.02.011>.
- Schauer, A.J., Kelson, J.R., Saenger, C., Huntington, K.W., 2016. Choice of 17O correction affects clumped isotope (Δ47) values of CO₂ measured with mass spectrometry. *Rapid Commun. Mass Spectrom.* 30, 2607–2616. <https://doi.org/10.1002/rcm.7743>.
- Seneviratne, S.I., Corti, T., Davin, E.L., Hirschi, M., Jaeger, E.B., Lehner, I., Orlowsky, B., Teuling, A.J., 2010. Investigating soil moisture–climate interactions in a changing climate: a review. *Earth Sci. Rev.* 99, 125–161. <https://doi.org/10.1016/j.earscirev.2010.02.004>.
- Sewall, J.O., Sloan, L.C., 2006. Come a little bit closer: a high-resolution climate study of the early Paleogene Laramide foreland. *Geology* 34, 81–84. <https://doi.org/10.1130/G22177.1>.
- Sikes, N.E., Ashley, G.M., 2007. Stable isotopes of pedogenic carbonates as indicators of paleoecology in the Plio-Pleistocene (upper Bed I), western margin of the Olduvai Basin, Tanzania. *J. Hum. Evol.* 53, 574–594. <https://doi.org/10.1016/j.jhevol.2006.12.008>.
- Smith, G.A., Wang, Y., Cerling, T.E., Geissman, J.W., 1993. *Pleistocene Climate in the Western United States*, pp. 691–694.
- Snell, K.E., Koch, P.L., Druschke, P., Foreman, B.Z., Eiler, J.M., 2014. High elevation of the ‘nevadaplano’ during the late cretaceous. *Earth Planet Sci. Lett.* 386, 52–63. <https://doi.org/10.1016/j.epsl.2013.10.046>.
- Snell, K.E., Thrasher, B.L., Eiler, J.M., Koch, P.L., Sloan, L.C., Tabor, N.J., 2013. Hot summers in the highhorn basin during the early paleogene. *Geology* 41, 55–58. <https://doi.org/10.1130/G33567.1>.
- Spencer, C., Kim, S.T., 2015. Carbonate clumped isotope paleothermometry: a review of recent advances in CO₂ gas evolution, purification, measurement and standardization techniques. *Geosci. J.* <https://doi.org/10.1007/s12303-015-0018-1>.
- Sprenger, M., McNamara, J.P., Buttle, J., Carey, S.K., Shatilla, N.J., Soulsby, C., 2018. Storage, mixing, and fluxes of water in the critical zone across northern environments inferred by stable isotopes of soil water. *Hydrol. Process.* 32, 1720–1737. <https://doi.org/10.1002/hyp.13135>.
- Suarez, D.L., Šimůnek, J., 1997. UNSATCHEM: unsaturated water and solute transport model with equilibrium and kinetic chemistry. *Soil Sci. Soc. Am. J.* 61, 1633. <https://doi.org/10.2136/sssaj1997.03615995006100060014x>.
- Suarez, M.B., Passey, B.H., Kaakinen, A., 2011. Paleosol carbonate multiple

- isotopologue signature of active East Asian summer monsoons during the late Miocene and Pliocene. *Geology* 39, 1151–1154. <https://doi.org/10.1130/G32350.1>.
- Tan, H., Liu, Z., Rao, W., Jin, B., Zhang, Y., 2017. Understanding recharge in soil-groundwater systems in high loess hills on the Loess Plateau using isotopic data. *Catena* 156, 18–29. <https://doi.org/10.1016/j.catena.2017.03.022>.
- Tang, J., Baldocchi, D.D., 2005. Spatial-temporal variation in soil respiration in an oak-grass savanna ecosystem in California and its partitioning into autotrophic and heterotrophic components. *Biogeochemistry* 73, 183–207. <https://doi.org/10.1007/s10533-004-5889-6>.
- Tang, K., Feng, X., 2001. The effect of soil hydrology on the oxygen and hydrogen isotopic compositions of plants' source water. *Earth Planet. Sci. Lett.* 185, 355–367. [https://doi.org/10.1016/S0012-821X\(00\)00385-X](https://doi.org/10.1016/S0012-821X(00)00385-X).
- Tobin, T.S., Wilson, G.P., Eiler, J.M., Hartman, J.H., 2014. Environmental change across a terrestrial Cretaceous–Paleogene boundary section in eastern Montana, USA, constrained by carbonate clumped isotope paleothermometry. *Geology* 42, 351–354. <https://doi.org/10.1130/G35262.1>.
- Újvári, G., Kele, S., Bernasconi, S.M., Haszpra, L., Novothny, Á., Bradák, B., 2019. Clumped isotope paleotemperatures from MIS 5 soil carbonates in southern Hungary. *Palaeogeogr. Palaeoclimatol. Palaeoecol.* 518, 72–81. <https://doi.org/10.1016/j.palaeo.2019.01.002>.
- Wang, Y., Cerling, T.E., Effland, W.R., 1993. Stable isotope ratios of soil carbonate and soil organic matter as indicators of forest invasion of prairie near Ames, Iowa. *Oecologia* 95, 365–369.
- Wang, Y., McDonald, E.V., Amundson, R.G., McFadden, L.D., Chadwick, O.A., 1996. An isotopic study of soils in chronological sequences of alluvial deposits, Providence Mountains, California. *Bull. Geol. Soc. Am.* 108, 379–391. [https://doi.org/10.1130/0016-7606\(1996\)108%3c0379:AISOSI%3e2.3.CO;2](https://doi.org/10.1130/0016-7606(1996)108%3c0379:AISOSI%3e2.3.CO;2).
- West, L.T., Wilding, L.P., Hallmark, C.T., 1988. Calciustolls in central Texas: II. Genesis of calcic and petrocalcic horizons. *Soil Sci. Soc. Am. J.* 52, 1731–1740. <https://doi.org/10.2136/sssaj1988.03615995005200060040x>.
- Young, M.H., Caldwell, T.G., Meadows, D.G., Fenstermaker, L.F., 2009. Variability of soil physical and hydraulic properties at the Mojave Global Change Facility, Nevada: implications for water budget and evapotranspiration. *J. Arid Environ.* 73, 733–744. <https://doi.org/10.1016/j.jaridenv.2009.01.015>.
- Zamanian, K., Pustovoytov, K., Kuzyakov, Y., 2016. Pedogenic carbonates: forms and formation processes. *Earth Sci. Rev.* 157, 1–17. <https://doi.org/10.1016/j.earscirev.2016.03.003>.